house Ryukyu and Han Chinese reference samples. Yamaguchi-Kabata *et al.* characterized the Japanese population structure using the genotypes for 140,387 SNPs in 7003 Japanese individuals, along with 60 European, 60 African, and 90 East-Asian individuals, in the HapMap project and found that the Japanese population is composed of 2 clusters (Hondo and Ryukyu) [36]. Hondo is the biggest island of Japan, and the island of Ryukyu is located in southern Japan. Also, we have 2nd or 3rd generation Chinese living in Japan, and Chinese present a different genetic population structure from Japanese. Therefore, we excluded samples belonging to Han Chinese or Ryukyu, and 938 cases and 2376 controls were considered for further analysis.

Cluster plots of SNPs were checked by visual inspection and SNPs with ambiguous calls were excluded. We excluded SNPs with a low genotyping rate (<90%), minor allele frequency less than 0.01 in either pediatric asthma cases or controls, or with Hardy-Weinberg equilibrium P value$<10^{-4}$ in controls. Finally, 450,326 SNPs were used for the GWAS. Details regarding the exact number of remaining SNPs after applying each quality control criterion are available in Table S1.

The genomic control inflation factor (λ_{GC}), defined as the median association test statistic across all SNPs divided by its expected value, was calculated by the method proposed by Devlin *et al.* [37]. GWAS and replication analyses were performed using the Cochran–Armitage trend test and χ^2 test. The meta-analysis was performed with the Mantel–Haenszel approach as a fixed-effects model [38]. All statistical findings were reported without correction. The results of GWAS were plotted with GWAS GUI v0.0.2 [39]. HLA-DP region was plotted with LocusZoom [40]. The power calculation was performed with Genetic Power Calculator [41]. Quantile-quantile (Q-Q) plot was plotted with ggplot2 package [42] in R version 2.10.0 (http://www.r-project.org/).

Imputation of genotypes in the DP region was performed with MACH version 1.0 [9] with 1000 Genome Project data (1000G 2010-6 release, http://www.sph.umich.edu/csg/yli/mach/download/1000G-2010-06.html).

HLA-DPA1 allele imputation

The HLA-DP region was in strong linkage disequilibrium and some DPB1 alleles were known to be linked with particular DPA1 alleles. First, we imputed HLA-DPA1 alleles by using the actual genotype data of samples obtained from Illumina HumanHap550v3/610-Quad (Illumina) and 1000 Genome Project data of Asian origin (JPT+CHB) (http://www.sph.umich.edu/csg/abecasis/MaCH/download/1000G-2010-06.html). The accuracy of the imputated data was confirmed by direct sequencing. The error rate of imputation was 1/352 (0.003).

Supporting Information

Table S1 Number of remaining SNPs after applying each quality control criterion.
(XLS)

Table S2 SNPs that are strong linkage disequilibrium ($r^2>0.9$) with rs987870.
(XLS)

Table S3 Association analysis for mite IgE sensitization.
(XLS)

Table S4 Genotyping data of the Japanese pediatric asthma GWAS.
(XLS)

Table S5 Characteristics of cases and controls.
(XLS)

Acknowledgments

We would like to thank the study participants for their participation of this study. We also thank for Dr. Toshio Abe, Dr. Hironobu Fukuda, and Dr. Mitsuhiro Nishida at Dokkyo Medical University, for collecting samples. We also thank Ms. Sumiko Ohnami (Division of Genetics, National Cancer Center Research Institute, Tokyo, Japan) for excellent technical support for genotyping and Mr. Shuhei Fukuda (Department of Allergy and Immunology, National Research Institute for Child Health and Development, Tokyo, Japan) for excellent technical support. We thank Naoharu Iwai (Department of Genomic Medicine, National Cerebral and Cardiovascular Center, Osaka, Japan) and Hitonobu Tomoike (Department of Preventive Cardiology, National Cerebral and Cardiovascular Center, Osaka, Japan) for providing genotype and phenotype information of Suita study. We thank Dr. Hirohiko Totsuka (Genetics Division, National Cancer Center Research Institute, and Bioinfomatics Group, Research and Development Center, Hitachi Government and Public Corporation System Engineering Ltd., Tokyo, Japan) for statistical analysis. We thank Dr. Saji at HLA laboratory for his technical support of HLA genotyping.

Author Contributions

Conceived and designed the experiments: E Noguchi, K Matsumoto. Performed the experiments: S Yoshihara, S-J Hong, Y Goto, T Asada, S Fujieda, N Hizawa, Y Nakamura, M Tamari, T Arinami, T Yoshida, Y Suzuki, H Sakamoto. Analyzed the data: H Saito, T Hirota, K Ochiai, M Sakashita. Contributed reagents/materials/analysis tools: Y Imoto, F Kurosaka, A Akasawa, N Shimojo, Y Kohno, N Kanno, Y Yamada, M-J Kang, J-W Kwon, F Yamashita, K Inoue, H Hirose, I Saito, T Sakamoto, H Masuko, I Nomura. Wrote the paper: E Noguchi, K Matsumoto.

References

1. Kusunoki T, Morimoto T, Nishikomori R, Yasumi T, Heike T, et al. (2009) Changing prevalence and severity of childhood allergic diseases in kyoto, Japan, from 1996 to 2006. Allergol Int 58: 543–548.
2. Pawankar R, Bunnag C, Chen Y, Fukuda T, Kim YY, et al. (2009) Allergic rhinitis and its impact on asthma update (ARIA 2008)–western and Asian-Pacific perspective. Asian Pac J Allergy Immunol 27: 237–243.
3. Moffatt MF, Kabesch M, Liang L, Dixon AL, Strachan D, et al. (2007) Genetic variants regulating ORMDL3 expression contribute to the risk of childhood asthma. Nature 448: 470–473.
4. Himes BE, Hunninghake GM, Baurley JW, Rafaels NM, Sleiman P, et al. (2009) Genome-wide association analysis identifies PDE4D as an asthma-susceptibility gene. Am J Hum Genet 84: 581–593.
5. Hancock DB, Romieu I, Shi M, Sienra-Monge JJ, Wu H, et al. (2009) Genome-wide association study implicates chromosome 9q21.31 as a susceptibility locus for asthma in mexican children. PLoS Genet 5: e1000623. doi:10.1371/journal.pgen.1000623.
6. Sleiman PM, Flory J, Imielinski M, Bradfield JP, Annaiah K, et al. (2010) Variants of DENND1B associated with asthma in children. N Engl J Med 362: 36–44.
7. Li X, Howard TD, Zheng SL, Haselkorn T, Peters SP, et al. (2010) Genome-wide association study of asthma identifies RAD50-IL13 and HLA-DR/DQ regions. J Allergy Clin Immunol 125: 328–335 e311.
8. Moffatt MF, Gut IG, Demenais F, Strachan DP, Bouzigon E, et al. (2010) A large-scale, consortium-based genomewide association study of asthma. N Engl J Med 363: 1211–1221.
9. Li Y, Willer C, Sanna S, Abecasis G (2009) Genotype imputation. Annu Rev Genomics Hum Genet 10: 387–406.
10. Imoto Y, Enomoto H, Fujieda S, Okamoto M, Sakashita M, et al. (2010) S2554X mutation in the filaggrin gene is associated with allergen sensitization in the Japanese population. J Allergy Clin Immunol 125: 498–500 e492.
11. Huang HW, Lue KH, Wong RH, Sun HL, Sheu JN, et al. (2006) Distribution of allergens in children with different atopic disorders in central Taiwan. Acta Paediatr Taiwan 47: 127–134.

12. Shibasaki M, Noguchi E, Takeda K, Takita H (1997) Distribution of IgE and IgG antibody levels against house dust mites in schoolchildren, and their relation with asthma. J Asthma 34: 235–242.
13. Yu VC, Delsert C, Andersen B, Holloway JM, Devary OV, et al. (1991) RXR beta: a coregulator that enhances binding of retinoic acid, thyroid hormone, and vitamin D receptors to their cognate response elements. Cell 67: 1251–1266.
14. Caraballo L, Marrugo J, Jimenez S, Angelini G, Ferrara GB (1991) Frequency of DPB1*0401 is significantly decreased in patients with allergic asthma in a mulatto population. Hum Immunol 32: 157–161.
15. Choi JH, Lee KW, Kim CW, Park CS, Lee HY, et al. (2009) The HLA DRB1*1501-DQB1*0602-DPB1*0501 haplotype is a risk factor for toluene diisocyanate-induced occupational asthma. Int Arch Allergy Immunol 150: 156–163.
16. Choi JH, Lee KW, Oh HB, Lee KJ, Suh YJ, et al. (2004) HLA association in aspirin-intolerant asthma: DPB1*0301 as a strong marker in a Korean population. J Allergy Clin Immunol 113: 562–564.
17. Howell WM, Standring P, Warner JA, Warner JO (1999) HLA class II genotype, HLA-DR B cell surface expression and allergen specific IgE production in atopic and non-atopic members of asthmatic family pedigrees. Clin Exp Allergy 29 Suppl 4: 35–38.
18. Shibasaki M, Hori T, Shimizu T, Isoyama S, Takeda K, et al. (1990) Relationship between asthma and seasonal allergic rhinitis in schoolchildren. Ann Allergy 65: 489–495.
19. Ovsyannikova IG, Jacobson RM, Vierkant RA, O'Byrne MM, Poland GA (2009) Replication of rubella vaccine population genetic studies: validation of HLA genotype and humoral response associations. Vaccine 27: 6926–6931.
20. Ovsyannikova IG, Ryan JE, Jacobson RM, Vierkant RA, Pankratz VS, et al. (2006) Human leukocyte antigen and interleukin 2, 10 and 12p40 cytokine responses to measles: is there evidence of the HLA effect? Cytokine 36: 173–179.
21. Yoshitake S, Kimura A, Okada M, Yao T, Sasazuki T (1999) HLA class II alleles in Japanese patients with inflammatory bowel disease. Tissue Antigens 53: 350–358.
22. Varney MD, Valdes AM, Carlson JA, Noble JA, Tait BD, et al. (2010) HLA DPA1, DPB1 alleles and haplotypes contribute to the risk associated with type 1 diabetes: analysis of the type 1 diabetes genetics consortium families. Diabetes 59: 2055–2062.
23. Zhou X, Lee JE, Arnett FC, Xiong M, Park MY, et al. (2009) HLA-DPB1 and DPB2 are genetic loci for systemic sclerosis: a genome-wide association study in Koreans with replication in North Americans. Arthritis Rheum 60: 3807–3814.
24. Zino E, Frumento G, Marktel S, Sormani MP, Ficara F, et al. (2004) A T-cell epitope encoded by a subset of HLA-DPB1 alleles determines nonpermissive mismatches for hematologic stem cell transplantation. Blood 103: 1417–1424.
25. Kimura A, Kitamura H, Date Y, Numano F (1996) Comprehensive analysis of HLA genes in Takayasu arteritis in Japan. Int J Cardiol 54 Suppl: S61–69.
26. Thomsen SF, Duffy DL, Kyvik KO, Skytthe A, Backer V (2010) Relationship between type 1 diabetes and atopic diseases in a twin population. Allergy.
27. Tzeng ST, Hsu SG, Fu LS, Chi CS (2007) Prevalence of atopy in children with type 1 diabetes mellitus in central Taiwan. J Microbiol Immunol Infect 40: 74–78.
28. Plenge RM, Seielstad M, Padyukov L, Lee AT, Remmers EF, et al. (2007) TRAF1-C5 as a risk locus for rheumatoid arthritis–a genomewide study. N Engl J Med 357: 1199–1209.
29. Price AL, Patterson NJ, Plenge RM, Weinblatt ME, Shadick NA, et al. (2006) Principal components analysis corrects for stratification in genome-wide association studies. Nat Genet 38: 904–909.
30. Sladek R, Rocheleau G, Rung J, Dina C, Shen L, et al. (2007) A genome-wide association study identifies novel risk loci for type 2 diabetes. Nature 445: 881–885.
31. Hiura Y, Tabara Y, Kokubo Y, Okamura T, Miki T, et al. (2010) A genome-wide association study of hypertension-related phenotypes in a Japanese population. Circ J 74: 2353–2359.
32. Harada M, Nakashima K, Hirota T, Shimizu M, Doi S, et al. (2007) Functional polymorphism in the suppressor of cytokine signaling 1 gene associated with adult asthma. Am J Respir Cell Mol Biol 36: 491–496.
33. Hirota T, Suzuki Y, Hasegawa K, Obara K, Matsuda A, et al. (2005) Functional haplotypes of IL-12B are associated with childhood atopic asthma. J Allergy Clin Immunol 116: 789–795.
34. Sakashita M, Yoshimoto T, Hirota T, Harada M, Okubo K, et al. (2008) Association of serum interleukin-33 level and the interleukin-33 genetic variant with Japanese cedar pollinosis. Clin Exp Allergy 38: 1875–1881.
35. Kim HB, Kang MJ, Lee SY, Jin HS, Kim JH, et al. (2008) Combined effect of tumour necrosis factor-alpha and interleukin-13 polymorphisms on bronchial hyperresponsiveness in Korean children with asthma. Clin Exp Allergy 38: 774–780.
36. Yamaguchi-Kabata Y, Nakazono K, Takahashi A, Saito S, Hosono N, et al. (2008) Japanese population structure, based on SNP genotypes from 7003 individuals compared to other ethnic groups: effects on population-based association studies. Am J Hum Genet 83: 445–456.
37. Devlin B, Roeder K (1999) Genomic control for association studies. Biometrics 55: 997–1004.
38. Petitti D (2000) Meta-Analysis, Decision Analysis, and Cost-Effective Analysis Second Edition Second Edition Oxford university pres.
39. Chen W, Liang L, Abecasis GR (2009) GWAS GUI: graphical browser for the results of whole-genome association studies with high-dimensional phenotypes. Bioinformatics 25: 284–285.
40. Pruim RJ, Welch RP, Sanna S, Teslovich TM, Chines PS, et al. (2010) LocusZoom: regional visualization of genome-wide association scan results. Bioinformatics 26: 2336–2337.
41. Purcell S, Cherny SS, Sham PC (2003) Genetic Power Calculator: design of linkage and association genetic mapping studies of complex traits. Bioinformatics 19: 149–150.
42. Wickham H (2009) ggplot2: elegant graphics for data analysis Springer New York.

Crucial role for autophagy in degranulation of mast cells

Hiroko Ushio, PhD,[a] Takashi Ueno, PhD,[b] Yuko Kojima, PhD,[c] Masaaki Komatsu, PhD,[e,f] Satoshi Tanaka, PhD,[g] Akitsugu Yamamoto, PhD,[h] Yoshinobu Ichimura, PhD,[e] Junji Ezaki, PhD,[b] Keigo Nishida, PhD,[i] Sachiko Komazawa-Sakon, BD,[d] François Niyonsaba, PhD,[a] Tetsuro Ishii, PhD,[j] Toru Yanagawa, DDS, MD, PhD,[j] Eiki Kominami, MD, PhD,[b] Hideoki Ogawa, MD, PhD,[a] Ko Okumura, MD, PhD,[a,d] and Hiroyasu Nakano, MD, PhD[d] *Tokyo, Kawaguchi, Okayama, Nagahama, Yokohama, and Tsukuba, Japan*

Background: Autophagy plays a crucial role in controlling various biological responses including starvation, homeostatic turnover of long-lived proteins, and invasion of bacteria. However, a role for autophagy in development and/or function of mast cells is unknown.

Objective: To investigate a role for autophagy in mast cells, we generated bone marrow–derived mast cells (BMMCs) from mice lacking autophagy related gene *(Atg) 7*, an essential enzyme for autophagy induction.

Methods: Bone marrow–derived mast cells were generated from bone marrow cells of control and IFN-inducible *Atg7*-deficient mice, and morphologic and functional analyses were performed.

Results: We found that conversion of type I to type II light chain (LC3)-II, a hallmark of autophagy, was constitutively induced in mast cells under full nutrient conditions, and LC3-II localized in secretory granules of mast cells. Although deletion of *Atg7* did not impair the development of BMMCs, $Atg7^{-/-}$ BMMCs showed severe impairment of degranulation, but not cytokine production on FcεRI cross-linking. Intriguingly, LC3-II but not LC3-I was co-localized with CD63, a secretory lysosomal marker, and was released extracellularly along with degranulation in $Atg7^{+/+}$ but not $Atg7^{-/-}$ BMMCs. Moreover, passive cutaneous anaphylaxis reactions were severely impaired in mast cell-deficient WBB6F1-W/W^V mice reconstituted with $Atg7^{-/-}$ BMMCs compared with $Atg7^{+/+}$ BMMCs.

Conclusion: These results suggest that autophagy is not essential for the development but plays a crucial role in degranulation of mast cells. Thus, autophagy might be a potential target to treat allergic diseases in which mast cells are critically involved.
(J Allergy Clin Immunol 2011;127:1267-76.)

Key words: Mast cell, autophagy, CD63, degranulation, p62, light chain 3 (LC3)

Autophagy is an evolutionarily conserved bulk degradation system in all eukaryotes that controls the clearance and reuse of intracellular constituents and is important for the maintenance of amino acid pools essential for survival.[1,2] This is initiated by the process in which organelles and cytosolic components are sequestered in double-membraned vesicles (so-called *autophagosomes*) and then delivered to lysosomes, where the autophagic cargo is degraded.[2] Yeast genetic screening studies have identified a variety of essential components of autophagy machinery, called autophagy related gene *(Atg)* genes, that are phylogenetically highly conserved. Among them, a mammalian counterpart of *Atg8*, light chain (LC)–3 localizes on autophagosomes through conversion of LC3-I to LC3-II by its C-terminal lipidification in an *Atg5*-dependent and *Atg7*-dependent fashion.[1,2] Although LC3-I diffusely distributes in cytoplasm, LC3-II shows a punctuate distribution. Accumulating studies using *Atg5*-deficient or *Atg7*-deficient mice have revealed that autophagy controls a variety of biological responses including aging, development, neurodegenerative diseases, intracellular bacterial infection, and cancer.[1,2] Intriguingly, autophagy has been shown to be critically involved in the packaging of antimicrobial peptides into granules in Paneth cells, thereby promoting efficient export of microbial peptides into the lumen of the gut.[3-5] Moreover, autophagy is also involved in the homeostasis of pancreatic β cells through degradation of toxic cytoplasmic components, such as damaged organelles and ubiquitinylated proteins.[6,7]

Mast cells express high-affinity receptors for IgE (FcεRI) on the cell surface and are able to release histamine, leukotriene C_4 (LTC_4), and other preformed chemical mediators on cross-linking of FcεRI receptors by polyvalent antigen, thereby playing a crucial role in allergic inflammatory reactions.[8,9] Mast cells are also involved in protection of the host from bacterial infection through production of TNF-α in response to bacteria components, such as LPS.[10-12] Most of these functions of mast cells are mediated by regulated exocytosis of specific secretory granules that are induced by antigen stimulation. Secretory granules in mast cells are considered to be secretory lysosomes that bridge the secretory and endocytic pathways. Selective transport of granular contents to granules of mast cells is considered to be regulated by synaptotagmins, mammalian homologue of Caenorhabditis elegans unc (Munc) 13-14, and rab27a.[13] However, the detailed mechanisms underlying sorting of granular contents to granules, and

From [a]the Atopy (Allergy) Research Center, [b]the Department of Biochemistry, [c]the Division of Biomedical Imaging Research, and [d]the Department of Immunology, Juntendo University School of Medicine, Tokyo; [e]the Laboratory of Frontier Science, Tokyo Metropolitan Institute of Medical Science; [f]PRESTO, Japan Science and Technology Corp, Kawaguchi; [g]the Department of Immunochemistry, Division of Pharmaceutical Sciences, Okayama University Graduate School of Medicine, Dentistry, and Pharmaceutical Sciences; [h]the Department of Cell Biology, Faculty of Bio-Science, Nagahama Institute of Bio-Science and Technology; [i]the Laboratory for Cytokine Signaling, RIKEN Research Center for Allergy and Immunology, Yokohama; and [j]the Graduate School of Comprehensive Human Sciences, University of Tsukuba.

Supported in part by grants-in-aid for the "High-Tech Research Center" Project for Private Universities; a matching fund subsidy from the Ministry of Education, Culture, Sports, Science and Technology, Japan, and Scientific Research (B) and (C) from the Japan Society for the Promotion of Science; the Science Research Promotion Fund from the Promotion and Mutual Aid Corporation for Private Schools of Japan; Scientific Research on Innovative Areas; MEXT, Japan; the Takeda Science Foundation; and the Astellas Foundation for Research on Metabolic Disorders.

Disclosure of potential conflict of interest: The authors have declared that they have no conflict of interest.

Received for publication May 6, 2010; revised November 25, 2010; accepted for publication December 15, 2010.

Available online February 18, 2011.

Reprint requests: Hiroko Ushio, PhD, or Hiroyasu Nakano, MD, PhD, Atopy Research Center or Department of Immunology, Juntendo University School of Medicine, 2-1-1 Hongo, Bunkyo-ku, Tokyo 113-8421, Japan. E-mail: hushio@juntendo.ac.jp or hnakano@juntendo.ac.jp.

0091-6749/$36.00

doi:10.1016/j.jaci.2010.12.1078

Abbreviations used

Atg: Autophagy related gene
BM: Bone marrow
BMMC: Bone marrow–derived mast cell
DC: Dendritic cell
FcεRI: High affinity receptor for IgE
GM-CSF: Granulocyte macrophage colony-stimulating factor
GFP: Green fluorescence protein
LC3: Light chain 3
LC3-I: Type I light chain 3
LC3-II: Type II light chain 3
LTC_4: Leukotriene C_4
M-CSF: Macrophage colony-stimulating factor
MFI: Mean fluorescence intensity
MVBs: Multivesicular bodies
PCA: Passive cutaneous anaphylaxis
PMA: Phorbol 12-myristate 13-acetate
Poly I:C: Polyinosinic-polycytidylic acid
SCF: Stem cell factor
siRNA: Small interfering RNA
SNARE: Soluble N-ethylmaleimide–sensitive factor attachment protein receptor

regulated exocytosis of granular contents by specific soluble N-ethylmaleimide–sensitive factor attachment protein receptor (SNARE), are not fully understood.[14] Because we found that conversion of LC3-I to LC3-II was constitutively induced in bone marrow (BM)–derived mast cells (BMMCs) under full nutrient conditions, we investigate a contribution of autophagy to the development and/or function of mast cells by using IFN-inducible *Atg7*-deficient mice.

METHODS

Mice

Atg7$^{Flox\ (F)/Flox\ (F)}$, *Atg7*$^{F/F}$*:Mx*, *Atg7*$^{F/F}$*:Mx:p62*$^{+/-}$, and *Atg7*$^{F/F}$*:Mx:p62*$^{-/-}$ mice were described previously.[15,16] Green fluorescence protein *(Gfp)-Lc3* transgenic mice were described elsewhere.[17] WBB6F1-+/+, WBB6F1-*W/W*^{V}, and C57BL/6 mice were purchased from Japan Clea (Tokyo, Japan). To induce deletion of *Atg7* gene, 8-week-old to 12-week-old *Atg7*$^{F/F}$*:Mx*, *Atg7*$^{F/F}$*:Mx:p62*$^{+/-}$, and *Atg7*$^{F/F}$*:Mx:p62*$^{-/-}$ mice were injected with 300 μg polyinosinic-polycytidylic acid (poly I:C; Sigma-Aldrich, Tokyo, Japan) 3 times every other day. At 2 weeks after the first poly I:C injection, BM cells from indicated genotyped mice were prepared as described and used for induction of BMMCs. In parallel experiments, *Mx-cre* negative flox mice were similarly injected with poly I:C, and BM cells were used to generate control BMMCs. Deletion of floxed alleles of *Atg7* genes was confirmed by PCR using BM cells or BMMCs. All experiments were performed according to the guidelines approved by the Institutional Animal Experiments Committee of Juntendo University School of Medicine.

Antibodies

Anti-GFP (Medical and Biological Laboratories [MBL], Nagoya, Japan), anti-LC3 (MBL), anti–β-actin (Sigma-Aldrich), anti-CD63 (MBL), antiubiquitin (MBL), anti–c-kit (BD Bioscience, Franklin Lakes, NJ), anti-FcεRI (eBioscience, San Diego, Calif), and anti-p62 (Stressgen, Brussels, Belgium) were purchased from indicated sources. Rabbit anti-LC3 antibody was generated and described previously.[15]

Cells

Bone marrow–derived mast cells were generated as previously described.[10] Briefly, BM cells were cultured in RPMI 1640 medium (Sigma-Aldrich) supplemented with 10% heat-inactivated FCS, 100 μmol/L 2-mercaptoethanol, 10 μmol/L minimum essential medium-nonessential amino acids, 100 U/mL penicillin, 100 μg/mL streptomycin, and 10 ng/mL murine IL-3 (Peprotech, Rocky Hill, NJ), or IL-3 + 10 or 100 ng/mL murine stem cell factor (SCF; Peprotech), for 5 to 8 weeks. After 5 weeks of culture, more than 98% of cells that were positive for both c-kit and FcεRI on the cell surface by flow cytometry and Diff-Quick staining were considered to be mature mast cells. A human mast cell line, laboratory of allergic diseases (LAD)2 cells (provided by Dr Arnold Kirshenbaum), were maintained as described previously.[18] Generation of macrophage colony-stimulating factor (M-CSF)–induced macrophages, granulocyte macrophage colony-stimulating factor (GM-CSF)–induced dendritic cells (DCs), and Flt3-induced DCs was described previously.[19]

Expression vectors

A lentiviral expression vector for Cherry fused to LC3 (Cherry-LC3) was generated as a standard method. Briefly, a full-length fragment of human LC3 was generated by PCR using pEGFP-LC3 (provided by Dr Isei Tanida) as a template, and subcloned into pmCherry-C1 (Clontech). Then, a Cherry-LC3 fragment was transferred into a lentiviral vector, CSII-EF-MCS (provided by Dr Hiroyuki Miyoshi), and designated plenti-Cherry-LC3. pCR-Cherry-LC3 was constructed by inserting a Cherry-LC3 fragment into pCR-3 (Invitrogen, Carlsbad, Calif). An expression vector for CD63-GFP was generated by subcloning murine CD63 into pEGFP-N1 (Clontech, Mountain View, Calif).

Generation of BMMCs stably expressing Cherry-LC3

Production of *Lentivirus* and infection of cells with *Lentivirus* were described elsewhere.[20] Briefly, 293T cells were transiently transfected with plenti-mCherry-LC3 along with packaging vectors, pCAG-HIV-gp, and pCMV-VSV-G-RSV-REV. At 48 hours after transfection, culture supernatants were collected and used for infection. BMMCs were incubated with the culture supernatants containing *Lentivirus* for 48 hours and then used for experiments.

Transient transfection of BMMCs

Bone marrow–derived mast cells were transiently transfected with expression vectors for pCR-Cherry-LC3 and pEGFP-CD63 by using a Nucleofector (Amaxa; Program Y-01, Solution V, Lonsa Group Ltd, Basel, Switzerland). At 24 hours after transfection, cells were used for subsequent experiments.

Knockdown of *Atg12* by small interfering (si) RNA

Wild-type BMMCs were transfected with control or *Atg12* siRNA (Applied Biosystems Japan, Tokyo, Japan) by using the Nucleofector (Amaxa; Program T-30, Solution V). Gene silencing efficiency was determined by quantitative (q)PCR. BMMCs were used for experiments 24 hours after transfection.

Degranulation of mast cells

Bone marrow–derived mast cells were sensitized with 1 μg/mL anti-trinitrophenol (TNP) IgE mAb (clone IgE-3; BD Biosciences) for 1 hour and then suspended at 1×10^6 cells/mL in Tyrode buffer containing 0.1% BSA. Cells were stimulated with indicated concentrations of anti-IgE antibody (BD Biosciences) or 1.6 nmol/L phorbol 12-myristate 13-acetate (PMA) plus 1 μmol/L ionomycin (Sigma-Aldrich) for 40 minutes at 37°C unless otherwise indicated. Degranulation of mast cells was determined by β-hexosaminidase and histamine release as described previously.[10] Degranulation was expressed as net percent release of β-hexosaminidase ([OD: stimulated – unstimulated/OD: total lysate – unstimulated] × 100%). There were no significant differences in the spontaneous release of β-hexosaminidase from *Atg7*$^{F/F}$-BMMCs and *Atg7*$^{\Delta BM}$-BMMCs (results; means ± SD; 10.007 ± 2.105% and 10.649 ± 1.262%, respectively). Concentrations of histamine in the same supernatants were determined by histamine competitive ELISA kit (Oxford Biomedical Research, Inc, Rochester Hills, Mich) according to the manufacturer's instructions, and degranulation was expressed as percent release of histamine as described in β-hexosaminidase.

Western blotting

Bone marrow–derived mast cells were untreated or stimulated as described. After stopping the reaction by adding ice-cold PBS, sample buffer containing SDS was directly added to the pellets, followed by brief sonication. Then, lysates were subjected to SDS-PAGE and transferred onto polyvinylidene difluoride membranes (Millipore, Billerica, Mass). In some experiments, supernatants after removal of degranulated cells were further centrifuged at 100,000*g* for 1 hour to obtain the granule pellets. Sample buffer was added to the pellets and subjected to SDS-PAGE. The membranes were analyzed by immunoblotting with indicated antibodies, followed by horseradish peroxidase–conjugated respective secondary anti-immunoglobulin antibodies. The membranes were developed with the Enhanced Chemiluminescence Western Blotting Detection System Plus (GE Healthcare Life Sciences, Tokyo, Japan).

Confocal microscopy

Bone marrow–derived mast cells were plated onto 12 wells containing 60-mm dishes (Ibidi GmbH, Munich, Germany) pretreated with poly-L-lysine (Sigma-Aldrich) and attached to dishes by centrifugation. Then, cells were fixed with 4% paraformaldehyde in PBS for 30 minutes and permeabilized with 50 μg/mL digitonin-PBS for 10 minutes. Cells were immunostained with anti-LC3, antiubiquitin, and anti-p62 antibodies in 1% BSA-Tris-buffered saline for 1 hour and were visualized with Alexa 488–conjugated or 594-conjugated secondary antibodies (Invitrogen). Confocal microscopy was performed on an FV1000 (Olympus, Tokyo, Japan). Pictures were analyzed by FV10-ASW (Olympus).

Transmission electron microscopy

Bone marrow–derived mast cells were prepared from wild-type C57BL/6, $Atg7^{F/F}$, and $Atg7^{F/F}$*:Mx* mice. To induce starvation, wild-type BMMCs were cultured in HBSS (+) without FCS for 2 hours. Cells were serially fixed with 2% glutaraldehyde in PBS for 2 hours and then with 2% osmium tetroxide (O_sO_4) for 2 hours before embedding in Epon 812. Thin sections were prepared by using a MT-5000 ultramicrotome (Dupont, Newtown, Mass) stained with uranyl acetate followed by lead citrate, and then observed on a JEM1230 electron transmission microscope (JEOL, New York, NY).

Measurement of translocation of CD63

Bone marrow–derived mast cells were sensitized as described and stimulated with TNP-BSA (1 ng/mL; LSL Co, Ltd, Tokyo, Japan) for 30 minutes at 37°C. The reaction was stopped with ice-cold PBS and fixed in 4% paraformaldehyde. Cells were stained with anti-CD63 antibody, followed by fluorescein isothiocyanate–conjugated rabbit antirat IgG antibody (ICN/Cappel, Costa Mesa, Calif), analyzed by FACS Caliber (BD Biosciences). The ratios of mean fluorescence intensities (MFIs) of CD63 on antigen-stimulated and unstimulated BMMCs were calculated.

Reconstitution of skin mast cells in WBB6F1-*W/W^v* mice with $Atg7^{F/F}$-BMMCs and $Atg7^{\Delta BM}$-BMMCs and passive cutaneous anaphylaxis reactions

Skin mast cells in ears of mast cell–deficient *W/W^v* mice were reconstituted by intradermal injection of $Atg7^{F/F}$-BMMCs or $Atg7^{\Delta BM}$-BMMCs. Six weeks after injection, reconstitution of skin mast cells was determined by Toluidine blue, or Alcian blue and Safranin staining of formalin-fixed tissue sections. To induce passive cutaneous anaphylaxis (PCA) reactions, mice were sensitized by intradermal injection of 4 μg anti-TNP IgE (clone IgE-3) or saline into ears of reconstituted mice. Two hours after IgE sensitization, 500 μL 0.5% Evans blue containing 100 μg TNP-BSA (LSL Co, Ltd) was injected intravenously. Ears were removed at 30 minutes after injection, and the amounts of dye in ears were measured as previously described.[10]

Statistical analysis

Statistical analysis was performed by unpaired Student *t* test. $P < .05$ was considered to be statistically significant.

RESULTS

Autophagy is constitutively induced in mast cells

To investigate whether autophagy may participate in the development and/or function of mast cells, we first examined whether autophagy is induced in wild-type BMMCs. Along with induction of autophagy, LC3-I is converted to LC3-II, and LC3-II becomes anchored to membrane of autophagosomes, thereby displaying a punctate distribution in the cytoplasm.[1,2] Intriguingly, we found that LC3-II was abundantly expressed in a melanoma cell line, BMMCs, and GM-CSF–induced DCs, but not freshly prepared BM cells, M-CSF–induced macrophages, or Flt3 ligand–induced DCs (Fig 1, *A*). We next performed confocal microscopic analysis to test whether LC3 displays a punctate distribution in BMMCs. To visualize localization of LC3, we analyzed 3 different BMMCs including BMMCs stably expressing Cherry-LC3, BMMCs from *Gfp-Lc3* transgenic mice that constitutively and ubiquitously express GFP-LC3 protein, and BMMCs stained with anti-LC3 antibody. In these all BMMCs, LC3 displayed a punctate distribution (Fig 1, *B*). Notably, although LC3 diffusely distributed in freshly prepared BM cells, numbers of LC3-positive dotlike structures and conversion of LC3-I to LC3-II were gradually increased along with maturation of BMMCs (see this article's Fig E1 in the Online Repository at www.jacionline.org). Moreover, we found that LC3 showed a punctate distribution, and conversion of LC3-I to LC3-II was constitutively induced in IL-3 + SCF-induced BMMCs, freshly isolated peritoneal MCs, and a human mast cell line, LAD2 cells (Fig 1, *C* and *D*). Considering that IL-3 + high concentrations of SCF (100 ng/mL) still induced autophagy in BMMCs (data not shown), it is unlikely that autophagy is induced in BMMCs because of poor nutrition conditions during culture. Together, autophagy is constitutively induced in MCs even under full nutrient conditions.

Given that autophagy was constitutively induced in MCs, we next tested whether autophagosome or autophagosome-like structures are detected in BMMCs. Transmission electron microscopic analysis of BMMCs revealed that there were a large number of granules filled with electron-dense materials and/or small vesicles, the latter reminiscent of multivesicular bodies (MVBs) (Fig 1, *E*). Notably, these granules were not identical to autophagosomes that usually sequestrate cytoplasmic components by isolation membrane and display double-membrane vesicles.[1,2] However, consistent with many studies using a variety of cells, typical autophagosomes were indeed induced in BMMCs under starved conditions (Fig 1, *E*, *right panel*). Collectively, these results suggest that LC3-II localizes in granules as well as autophagosomes.

Normal development of BMMCs from *Atg7*-deficient mice

Autophagy was constitutively induced in BMMCs, prompting us to test whether autophagy may play a role in the development of mast cells. Given that $Atg7^{-/-}$ mice died soon after birth,[15,21] we generated BMMCs from BM cells of IFN-inducible *Atg7*-deficient ($Atg7^{F/F}$*:Mx*) mice. After poly I:C injection, floxed alleles of *Atg7* were completely deleted in BM from $Atg7^{F/F}$*:Mx* mice but not control $Atg7^{F/F}$ mice (Fig 2, *A*). We referred to poly I:C-injected $Atg7^{F/F}$*:Mx* mice as $Atg7^{\Delta BM}$ mice hereafter. Importantly, after a 4-week culture, floxed alleles of *Atg7* were still deleted in BMMCs from $Atg7^{\Delta BM}$ mice (Fig 2, *A*), and conversion of LC3-I to LC3-II was completely blocked in BMMCs from $Atg7^{\Delta BM}$ mice (Fig 2, *B*).

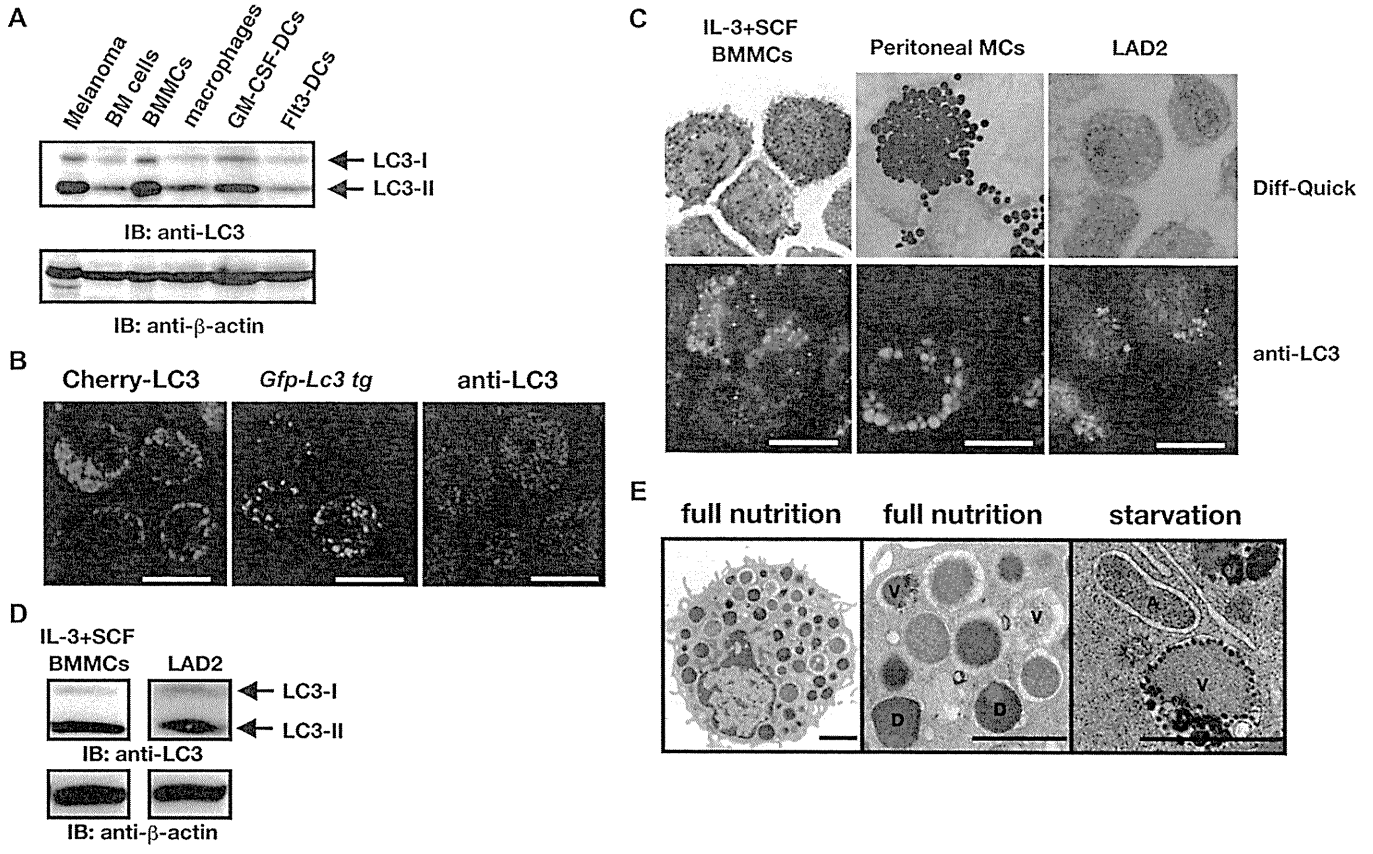

FIG 1. Autophagy is constitutively induced in mast cells. **A and D,** Conversion of LC3-I to LC3-II was analyzed by immunoblotting *(IB)*. **B,** Confocal microscopic analysis of BMMCs stably expressing Cherry-LC3, BMMCs derived from *Gfp-Lc3* transgenic mice, or BMMCs stained with anti-LC3 antibody. Scale bars, 10 μm. **C,** IL-3 + SCF-induced BMMCs, peritoneal mast cells, and human LAD2 mast cells were stained with anti-LC3 antibody or Diff-Quick. Scale bars, 10 μm. **E,** BMMCs cultured in indicated conditions were analyzed by transmission electron microscopy. *D,* Electron-dense granule; *V,* multivesicular-like granule; *A,* autophagosome. Scale bars, 500 nm.

After a 4-week culture, almost 98% of cultured cells from $Atg7^{\Delta BM}$ as well as $Atg7^{F/F}$ mice became positive for both c-kit and FcεRI, and expression levels of FcεRI were not different between $Atg7^{F/F}$-BMMCs and $Atg7^{\Delta BM}$-BMMCs (Fig 2, *C*). Thus, these cells were considered to be mature BMMCs. In addition, the total numbers of $Atg7^{\Delta BM}$-BMMCs were comparable to those of $Atg7^{F/F}$-BMMCs (Fig 2, *D*). Moreover, Diff-Quick staining showed that staining intensities of intracellular granules of $Atg7^{\Delta BM}$-BMMCs were not significantly different from those of $Atg7^{F/F}$-BMMCs (Fig 2, *E*). Together, differentiation and proliferation of $Atg7^{\Delta BM}$-BMMCs appeared to be normal. However, LC3-I formed large aggregates in $Atg7^{\Delta BM}$-BMMCs because of a defect in conversion from LC3-I to LC3-II by *Atg7* gene deficiency, whereas LC3-II showed a punctate distribution in $Atg7^{F/F}$-BMMCs (Fig 2, *F*).

Autophagy plays a crucial role in FcεRI-induced degranulation by BMMCs

Because LC3-II appears to localize in granules, we examined whether degranulation is impaired in $Atg7^{\Delta BM}$-BMMCs. Interestingly, FcεRI-induced releases of both β-hexosaminidase and histamine were severely impaired in $Atg7^{\Delta BM}$-BMMCs, whereas total cellular contents of β-hexosaminidase and histamine were slightly reduced in $Atg7^{\Delta BM}$-BMMCs compared with $Atg7^{F/F}$-BMMCs (Fig 3, *A*). In sharp contrast, PMA/ionomycin–induced release of β-hexosaminidase and histamine by $Atg7^{\Delta BM}$-BMMCs was comparable to that by $Atg7^{F/F}$-BMMCs, suggesting that impairment of degranulation caused by deficiency of autophagy might be overcome by strong signals that induce degranulation (Fig 3, *A*). Notably, FcεRI-induced release of β-hexosaminidase and histamine was severely impaired in $Atg7^{\Delta BM}$-BMMCs at any time point after stimulation (see this article's Fig E2 in the Online Repository at www.jacionline.org), indicating that FcεRI-induced degranulation is not delayed in $Atg7^{\Delta BM}$-BMMCs compared with $Atg7^{F/F}$-BMMCs. We also observed similar impairment in degranulation in IL3 + SCF-induced $Atg7^{\Delta BM}$-BMMCs (Fig 3, *B*).

To substantiate further a contribution of the autophagy-dependent signaling pathway to degranulation of BMMCs, we tested whether knockdown of an autophagy-related gene other than *Atg7* could impair FcεRI-induced degranulation of BMMCs. Knockdown of *Atg12* gene (Fig 3, *C*), which is also essential for autophagosome formation, similarly impaired releases of β-hexosaminidase and histamine by BMMCs (Fig 3, *D*). These results further substantiate that *Atg7*-dependent and *Atg12*-dependent signaling pathways play a crucial role in degranulation of mast cells and exclude a possibility that *Atg7* may control degranulation by mast cells in an autophagy-independent fashion.

The signaling pathways leading to degranulation of BMMCs triggered by FcεRI cross-linking depend on phosphorylation of early signaling molecules and Ca^{2+} mobilization.[22] Thus, we next

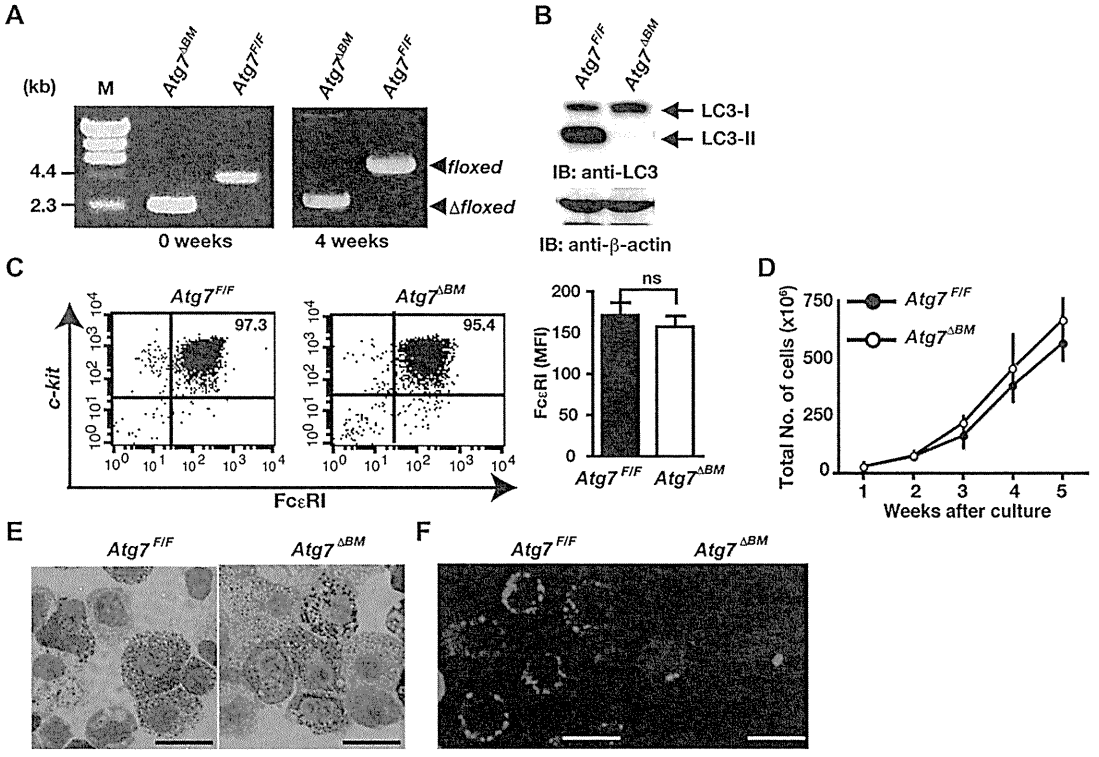

FIG 2. Normal development of BMMCs derived from IFN-inducible *Atg7*-deficient mice. **A,** Complete deletion of floxed alleles of *Atg7* gene of freshly prepared BM cells or 4-week-cultured BMMCs from $Atg7^{\Delta BM}$ mice was determined by PCR. *M,* Marker. **B,** Conversion of LC3-I to LC3-II was analyzed by immunoblotting *(IB).* **C,** $Atg7^{F/F}$-BMMCs and $Atg7^{\Delta BM}$-BMMCs were stained with anti–c-kit and anti-FcεRI antibodies and analyzed by flow cytometry. Results are representative of 6 independent experiments. MFIs of FcεRI expression on $Atg7^{F/F}$-BMMCs and $Atg7^{\Delta BM}$-BMMCs. Results are means ± SDs of 3 independent experiments. *ns,* Not significant. **D,** Total numbers of cells during development of BMMCs from $Atg7^{\Delta BM}$ mice are comparable to those from $Atg7^{F/F}$ mice. Results are means ± SDs of 3 independently prepared BMMCs. **E,** $Atg7^{F/F}$-BMMCs and $Atg7^{\Delta BM}$-BMMCs after 5 weeks of culture were stained with Diff-Quick. Scale bars, 20 μm. **F,** $Atg7^{F/F}$-BMMCs and $Atg7^{\Delta BM}$-BMMCs stably expressing Cherry-LC3 were analyzed by confocal microscopy. Scale bars, 10 μm.

investigated whether these signaling pathways are impaired in $Atg7^{\Delta BM}$-BMMCs. Ca^{2+} mobilization and phosphorylation of early signaling molecules including syk, phospholipase C-γ1, and gab2 were not impaired in $Atg7^{\Delta BM}$-BMMCs compared with $Atg7^{F/F}$-BMMCs (see this article's Fig E3 in the Online Repository at www.jacionline.org). Moreover, production of inflammatory cytokines such as IL-6 and TNF-α, generation of LTC_4, activation of the mitogen-activated protein kinases (MAPKs), or phosphorylation of inhibitor of NF-kappa B (IκB)α were not impaired in $Atg7^{\Delta BM}$-BMMCs (see this article's Fig E4 in the Online Repository at www.jacionline.org). These results suggest that deficiency of autophagy results in a relatively specific defect in degranulation, but not global dysfunction of mast cells.

LC3-II co-localizes with a secretory lysosomal marker, CD63, and upregulation of CD63 on cell surface is impaired in $Atg7^{\Delta BM}$-BMMCs on stimulation

Taken that FcεRI-induced degranulation, but not Ca^{2+} mobilization or phosphorylation of early signaling molecules, was impaired in $Atg7^{\Delta BM}$-BMMCs, we surmised that autophagy may play a role in granule maturation, translocation, or fusion of granules with the plasma membrane along with degranulation. A previous study has shown that a member of the tetraspanin family, CD63 (also known as lysosomal-associated membrane protein-3), localizes on granule membranes of basophils, mast cells, and platelets, and is considered to be a secretory lysosomal marker.[23] Moreover, expression of CD63 on cell surfaces is upregulated along with degranulation through granule-plasma membrane fusion.[22] Thus, we investigated whether LC3-II co-localizes with CD63. We transiently transfected expression vectors for GFP-CD63 and Cherry-LC3 into $Atg7^{F/F}$-BMMCs and $Atg7^{\Delta BM}$-BMMCs and analyzed intracellular localization by confocal microscopy. Intriguingly, LC3-II completely co-localized with CD63 in $Atg7^{F/F}$-BMMCs, but not in $Atg7^{\Delta BM}$-BMMCs, in which LC3-I formed large aggregates or diffusely distributed in the cytoplasm (Fig 4, *A*). Moreover, we also found that endogenous LC3-II partially co-localized with endogenous CD63 in BMMCs (Fig 4, *B*). We then tested whether FcεRI-induced upregulation of CD63 on cell surfaces is impaired in $Atg7^{\Delta BM}$-BMMCs. We sensitized BMMCs with anti-TNP-IgE, then stimulated them with TNP-BSA. Although surface expression of CD63 on $Atg7^{F/F}$-BMMCs was almost equivalent to $Atg7^{\Delta BM}$-BMMCs before stimulation, upregulation of CD63 on stimulation was lower in $Atg7^{\Delta BM}$-BMMCs compared with $Atg7^{F/F}$-BMMCs (Fig 4, *C*). Relative ratios of MFI of CD63 on stimulated/unstimulated $Atg7^{\Delta BM}$-BMMCs were substantially

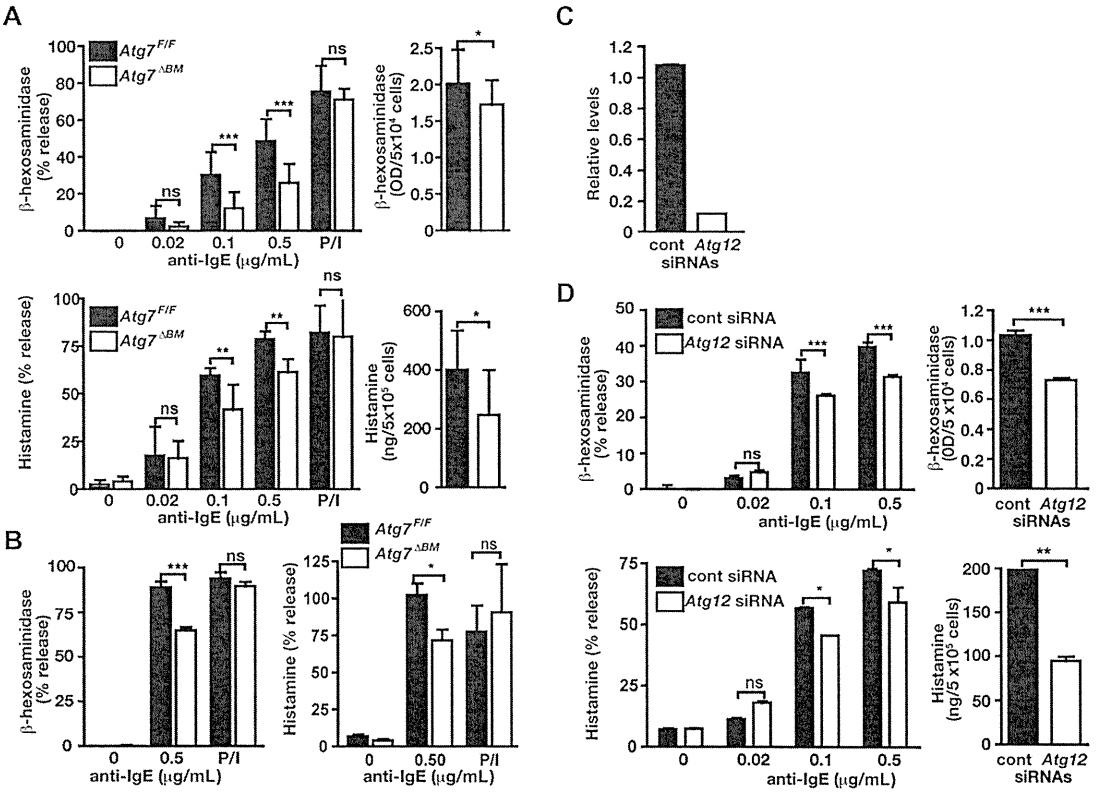

FIG 3. Autophagy plays a crucial role in FcεRI-induced degranulation by BMMCs. **A,** Release of β-hexosaminidase and histamine in culture supernatants and their total contents in cell lysates were measured. *P/I,* PMA/ionomycin. Results are means ± SDs of triplicate samples and pooled data of 9 to 10 independent experiments. **B,** FcεRI-induced degranulation is similarly impaired in IL-3 + SCF-induced $Atg7^{\Delta BM}$-BMMCs. **C,** Knockdown of *Atg12* by siRNA in wild-type BMMCs. Relative expression levels of *Atg12* mRNA were determined by qPCR. **D,** FcεRI-induced degranulation is impaired in *Atg12* knockdown BMMCs. Results are means ± SDs of 3 independent experiments, (**B** and **D**). $*P < .05$; $**P < .01$; $***P < .001$. *cont,* Control; *ns,* not significant.

decreased compared with those on $Atg7^{F/F}$-BMMCs (Fig 4, *C*). These results suggest that granule translocation or fusion of granules with the plasma membrane is partially impaired in $Atg7^{\Delta BM}$-BMMCs.

LC3-II is released extracellularly along with degranulation in $Atg7^{F/F}$-BMMCs, but this release is impaired in $Atg7^{\Delta BM}$ -BMMCs

Taken that LC3-II accumulated in granules and co-localized with CD63 (Fig 4, *A* and *B*), it would be intriguing to test whether LC3-II may be released into extracellular space like exosomes along with degranulation.[24] To visualize this process, we unstimulated or stimulated $Atg7^{F/F}$-BMMCs and $Atg7^{\Delta BM}$-BMMCs stably expressing Cherry-LC3, and then analyzed them by confocal microscopy. Although Cherry-LC3 showed a punctate distribution in the cytoplasm before stimulation, Cherry-LC3–positive signals were drastically diminished in $Atg7^{F/F}$-BMMCs after stimulation (Fig 5, *A, left panels*). More importantly, Cherry-LC3 was released into extracellular space along with degranulation (Fig 5, *A, left lower panel*). However, such release was not detected in $Atg7^{\Delta BM}$-BMMCs (Fig 5, *A, right lower panel*). To evaluate the contents of released LC3-II more quantitatively, we collected culture supernatants from untreated or stimulated $Atg7^{F/F}$-BMMCs and $Atg7^{\Delta BM}$-BMMCs and isolated the granule fractions by ultracentrifugation. We examined the contents of LC3-II in the granule fractions by Western blotting. Endogenous LC3-II was indeed detected in the released granule fractions from stimulated $Atg7^{F/F}$-BMMCs but not $Atg7^{F/F}$-BMMCs (Fig 5, *B*). Moreover, large amounts of CD63 were detected in the released granule fractions; however, such release of CD63 was significantly reduced in $Atg7^{\Delta BM}$-BMMCs (Fig 5, *B*). These results suggest that LC3-II–positive and CD63-positive granules are released extracellularly like exosomes.[24]

Formation of ubiquitin-positive and p62-positive inclusions in $Atg7^{\Delta BM}$-BMMCs

Recent studies have shown that inactivation of autophagy results in formation of large aggregates, culminating in the development of liver injury and neurodegeneration.[15,25,26] We have recently identified an adaptor protein, p62 (also known as A170 or SQSTM1 [Sequestosome 1]), that has been shown to be involved in various signaling pathways as a binding molecule to LC3.[16,27] Importantly, deletion of *p62* gene abolishes ubiquitin-positive aggregates and also ameliorates hepatitis of hepatocyte-specific *Atg7*-deficient mice.[16] To investigate further the mechanisms underlying impaired degranulation of $Atg7^{\Delta BM}$-BMMCs on stimulation, we first tested whether ubiquitin-positive and p62-positive aggregates were similarly observed in

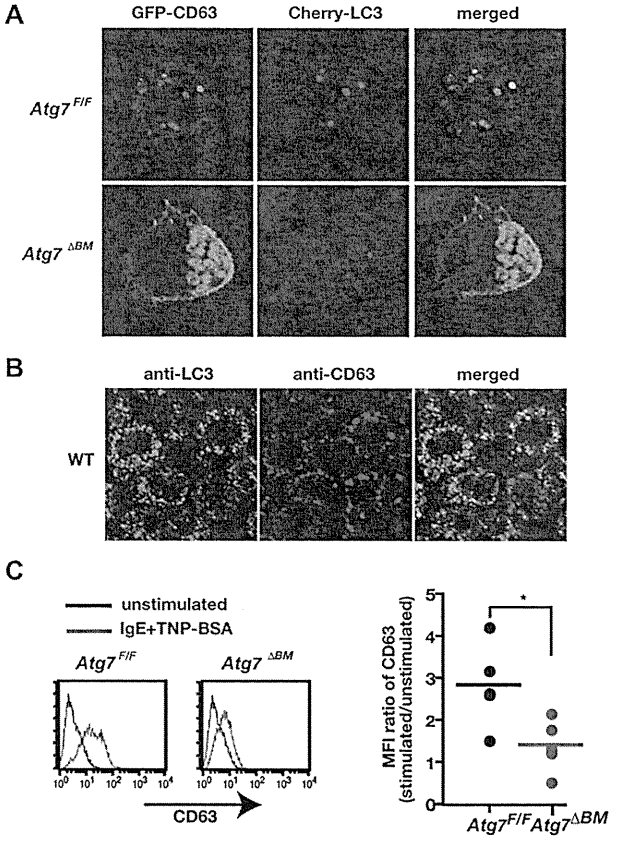

FIG 4. LC3 co-localizes with CD63 in $Atg7^{F/F}$-BMMCs but not $Atg7^{\Delta BM}$-BMMCs. **A,** BMMCs were cotransfected with indicated expression vectors and analyzed by confocal microscopy. Scale bars, 10 μm. **B,** Endogenous LC3 partially co-localizes with endogenous CD63. Wild-type *(WT)* BMMCs were stained with indicated antibodies and analyzed as in *A*. Scale bars, 10 μm. **C,** Upregulation of CD63 on cell surface is impaired in $Atg7^{\Delta BM}$-BMMCs. BMMCs were unstimulated or stimulated with TNP-BSA. Expression of CD63 on cell surfaces was analyzed by flow cytometry. Relative ratios of MFI of CD63 on cell surface of $Atg7^{F/F}$-BMMCs and $Atg7^{\Delta BM}$-BMMCs unstimulated or stimulated with TNP-BSA are shown. Results are means ± SDs of 4 independent experiments. $^*P < .05$.

$Atg7^{\Delta BM}$-BMMCs. LC3-I formed aggregates that completely merged with staining with anti-p62 and antiubiquitin antibodies in $Atg7^{\Delta BM}$-BMMCs (Fig 6, *A*). Expression levels of p62 were markedly increased in lysates of $Atg7^{\Delta BM}$-BMMCs compared with $Atg7^{F/F}$-BMMCs (Fig 6, *B*). FcεRI-induced activation of mast cells did not alter expression levels of p62 in $Atg7^{\Delta BM}$-BMMCs and $Atg7^{F/F}$-BMMCs. Moreover, transmission electron microscopy showed that amorphous and electron-thin substances accumulated in the cytoplasm of $Atg7^{\Delta BM}$-BMMCs, which might correspond to aggregates containing p62, LC3-I, and ubiquitinylated proteins (Fig 6, *C, lower panel*). However, such amorphous structures were not observed in $Atg7^{F/F}$-BMMCs (Fig 6, *C, upper panel*).

To test a possibility that large aggregates containing p62 could impair degranulation of $Atg7^{\Delta BM}$-BMMCs, we next generated BMMCs derived from *Atg7* and *p62*–double-deficient mice. Deletion of *p62* completely eliminated large ubiquitin-positive aggregates (see this article's Fig E5, *A,* in the Online Repository at www.jacionline.org), but FcεRI-induced degranulation was still impaired in $Atg7^{\Delta BM}$:$p62^{-/-}$-BMMCs (Fig E5, *B*). Together, these results suggest that impairment of FcεRI-induced release of β-hexosaminidase and histamine by $Atg7^{\Delta BM}$-BMMCs is not a result of accumulation of aggregates containing p62, LC3, and ubiquitinylated proteins.

Passive cutaneous anaphylaxis reactions were severely impaired in mast cell–deficient mice reconstituted with $Atg7^{\Delta BM}$-BMMCs

To demonstrate an *in vivo* relevance of autophagy in mast cells, we adoptively transferred $Atg7^{F/F}$-BMMCs and $Atg7^{\Delta BM}$-BMMCs into skins of mast cell–deficient WBB6F1-W/W^V mice. We assessed degranulation of reconstituted mast cells by PCA reactions. Although reconstitution efficiency of $Atg7^{\Delta BM}$-BMMCs was approximately 70% of those of $Atg7^{F/F}$-BMMCs (Fig 7, *A* and *B*), the PCA reaction was almost completely abolished in W/W^V mice reconstituted with $Atg7^{\Delta BM}$-BMMCs (Fig 7, *C*). Although we need to consider that a severe defect in PCA reaction is partly affected by lower numbers of reconstituted $Atg7^{\Delta BM}$-BMMCs that had slightly lower histamine contents, autophagy plays a crucial role in degranulation of mast cells *in vivo*.

DISCUSSION

In the current study, we found that autophagy was constitutively induced in mast cells. Confocal and transmission electron microscopic analysis revealed that LC3-II localized in CD63-positive secretory granules, some of which were reminiscent of MVBs, but not typical autophagosomes in BMMCs. Moreover, FcεRI-induced degranulation, but not cytokine production or LTC_4 generation, was severely impaired in $Atg7^{\Delta BM}$-BMMCs. Intriguingly, LC3-II was released into extracellular space along with degranulation in $Atg7^{F/F}$- but not $Atg7^{\Delta BM}$-BMMCs. Furthermore, PCA reactions were severely impaired in W/W^V mice reconstituted with $Atg7^{\Delta BM}$-BMMCs. Together, these findings show that autophagy plays a crucial role in degranulation of mast cells *in vitro* and *in vivo*.

One of the most important and unexpected findings in this study is that LC3-II accumulated in mast cell granules under full nutrient conditions and was released extracellularly along with degranulation (Fig 5). It is not likely that LC3-II normally anchored to isolation membranes of autophagosomes is released extracellularly through fusion of autophagosomes with the plasma membrane, because under these conditions, LC3-II should remain in the plasma membrane. One plausible interpretation would be that at least some portions of LC3-II–positive and CD63-positive granules may be initially generated from small vesicles that sequestrate a set of contents of secretory granules such as histamine and β-hexosaminidase (Fig 1, *E*). These small vesicles may eventually be engulfed by MVBs to become mature secretory granules. If that is the case, LC3-II anchored to membrane of small vesicles may be released into extracellular space through fusion of MVBs with the plasma membrane. Consistently, recent studies in yeast have shown that selective autophagy collects cargos that are subsequently engulfed by multivesicular endosomes, which eventually fuse with the plasma membrane to release its contents extracellularly.[28,29] Although this secretory pathway is called unconventional protein secretion,[30] our current study suggests for the first time a possible link between autophagy and the unconventional protein secretion pathway in degranulation of mast cells.

Mast cell exocytosis of secretory granules occurs by a highly regulated series of events, which is controlled by SNARE

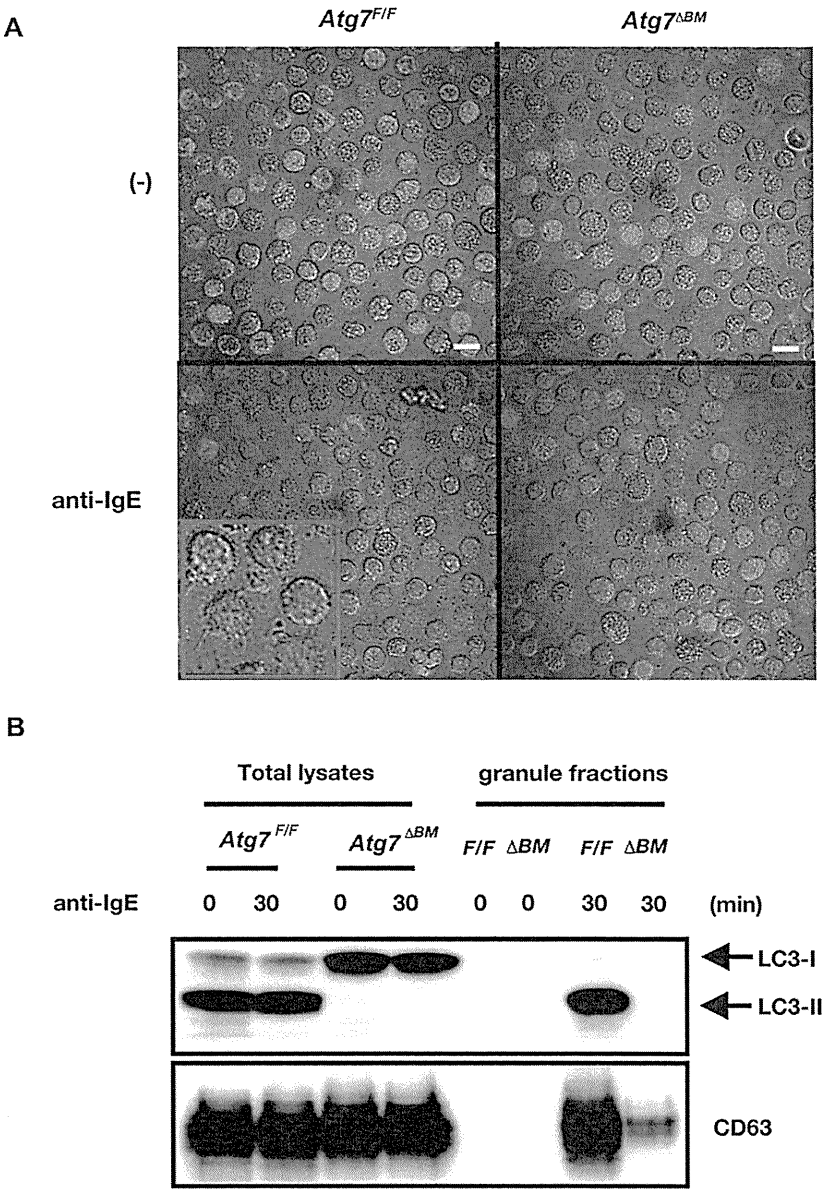

FIG 5. Extracellular release of LC3-II along with degranulation of BMMCs. **A,** BMMCs stably expressing Cherry-LC3 were untreated or stimulated with anti-IgE antibody and analyzed by confocal microscopy. *Red box* is enlarged image. Scale bars, 10 μm. **B,** LC3-II but not LC3-I is detected in the released granule fractions after stimulation. Cell lysates and the released granule fractions from untreated or stimulated BMMCs were analyzed by immunoblotting.

proteins.[14] Intriguingly, recent studies have shown that degranulation, but not cytokine or chemokine production, is impaired in mast cells deficient in vesicular-associated membrane protein 8, a member of the vesicular SNARE complex.[31,32] Similar to vesicular-associated membrane protein $8^{-/-}$ mast cells, degranulation, but not cytokine release or LTC_4 generation, was selectively impaired in $Atg7^{\Delta BM}$-BMMCs, further substantiating that degranulation and release of cytokines are differentially regulated by possibly different SNARE proteins. Given that MAPK activation was not impaired in autophagy-deficient BMMCs (Fig E4, *C* and *D*), lack of a defect in cytokine release and LTC_4 generation in autophagy-deficient BMMCs is consistent with previous studies, in which activation of the MAPK pathways are critically involved in this process. Partial impairment of upregulation of CD63 on cell surfaces in $Atg7^{\Delta BM}$-BMMCs suggested that autophagy may also be implicated in this process (Fig 4, *C*), although the detailed mechanisms have not been fully investigated. On the other hand, strong calcium signals are known to mobilize both secretory and conventional lysosomes in a variety of cell types.[33,34] Indeed, PMA/ionomycin–induced degranulation was not impaired in $Atg7^{\Delta BM}$-BMMCs (Fig 3, *A*). This suggests that deficiency of autophagy may be overcome by a strong signal such as PMA/ionomycin that may mobilize degranulation of both secretory and conventional lysosomes.[34]

Autophagy deficiency has been shown to induce degeneration of mitochondria, which results in impaired insulin secretion from pancreatic β cells in $Atg7^{-/-}$ mice because of decline in cellular ATP contents.[6,7] Given that optimal cellular ATP levels may be crucial

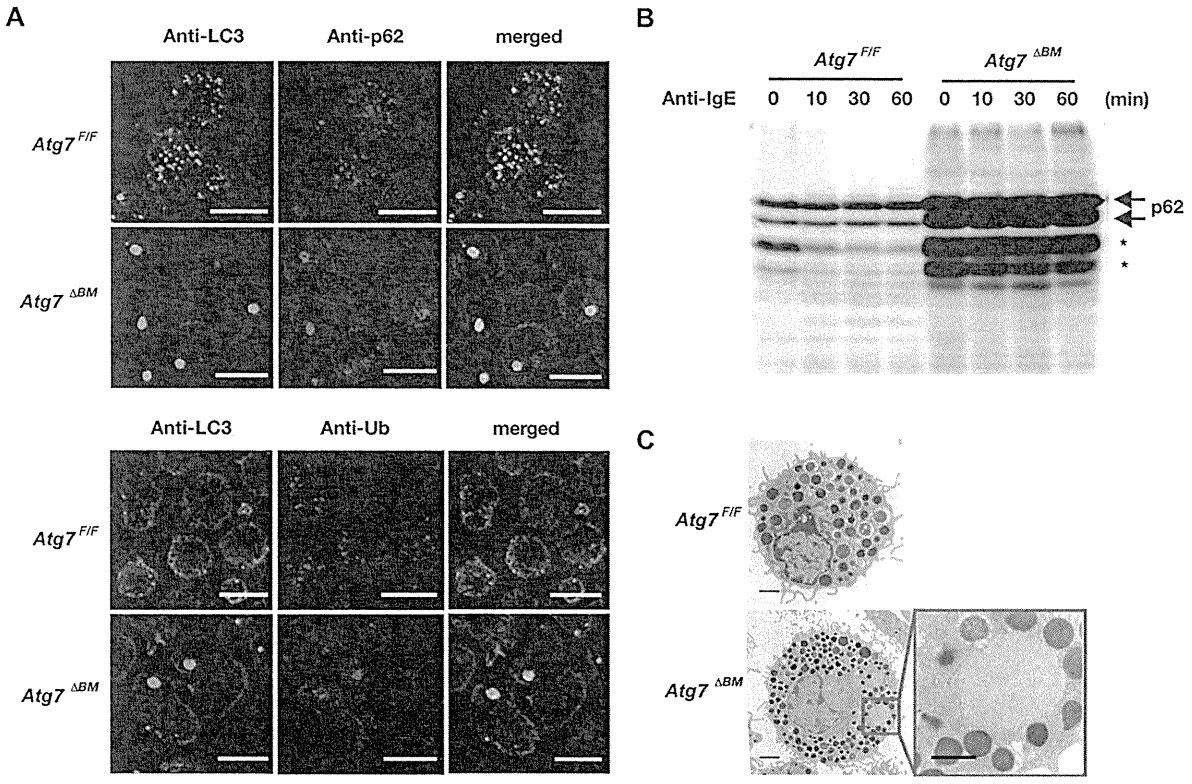

FIG 6. LC3-I, p62, and ubiquitinylated proteins form large aggregates in *Atg7*$^{\Delta BM}$-BMMCs. **A,** BMMCs were stained with indicated antibodies and analyzed by confocal microscopy *UB,* Ubiquitin. Scale bars, 10 μm. **B,** Accumulation of p62 in *Atg7*$^{\Delta BM}$-BMMCs was analyzed by immunoblotting. **C,** BMMCs were analyzed by transmission electron microscopy. Scale bar, 1 μm. *Red box* is enlarged image.

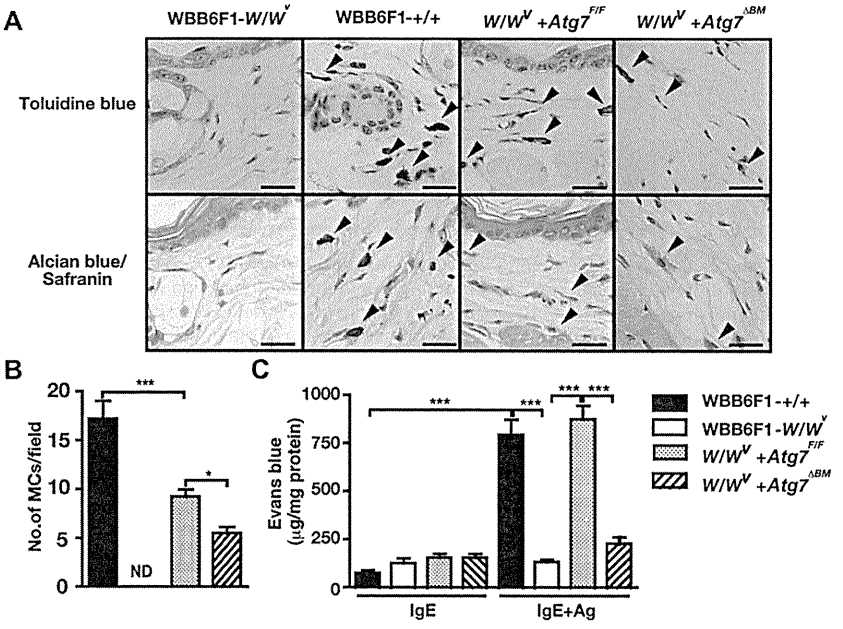

FIG 7. A severe impairment in PCA reactions in mast cell–deficient mice reconstituted with *Atg7*$^{\Delta BM}$-BMMCs. **A,** Skin (ear) sections from indicated mice were stained with Toluidine blue, or Alcian blue and Safranin. *Arrowheads* indicate mast cells. Scale bars, 20 μm. **B,** The numbers of skin mast cells in indicated mice. **C,** PCA reactions in indicated mice. Results are means ± SDs of 4 to 5 mice. *B and C,* *$P < .05$; ***$P < .001$. *Ag,* Antigen; *MC,* mast cell; *ND,* Not detected.

for activation of kinases involved in degranulation, we examined cellular ATP contents in $Atg7^{F/F}$-BMMCs and $Atg7^{\Delta BM}$-BMMCs. In contrast with our expectations, cellular ATP contents were increased in $Atg7^{\Delta BM}$-BMMCs compared with $Atg7^{F/F}$-BMMCs (data not shown). Although the reason cellular ATP contents were increased in $Atg7^{\Delta BM}$-BMMCs is currently unknown, these results suggest that impaired degranulation is not caused by a decline in cellular ATP contents in $Atg7^{\Delta BM}$-BMMCs.

A significant defect in PCA reactions in W/W^V mice reconstituted with $Atg7^{\Delta BM}$-BMMCs has clearly shown an *in vivo* relevance of autophagy in mast cells (Fig 7, *C*). Although mast cells appear to be promising targets to treat various allergic diseases including atopic dermatitis and asthma, we and others previously reported a crucial role for mast cells in protection of hosts from bacterial infection.[10-12] Therefore, a strategy to inhibit global function of mast cells might cause serious side effects through exacerbating bacterial infections. Taken that inhibition of autophagy might selectively impair FcεRI-induced degranulation, but not cytokine production by mast cells, autophagy might be a potential target to treat allergic diseases by selective suppression of antigen-induced degranulation of mast cells.

We thank N. Mizushima, I. Tanida, H. Miyoshi, H. Suzuki, H. Ohno, K. Waguri, and M. Koike for providing reagents and helpful discussions. We also thank M. Yoshida, J. Nakamoto, and K. Takahashi for support of transmission electron microscopy.

Clinical implications: Autophagy might be a potential target to treat allergic diseases in which mast cells are critically involved.

REFERENCES

1. Mizushima N, Levine B, Cuervo AM, Klionsky DJ. Autophagy fights disease through cellular self-digestion. Nature 2008;451:1069-75.
2. Levine B, Kroemer G. Autophagy in the pathogenesis of disease. Cell 2008;132:27-42.
3. Cadwell K, Liu JY, Brown SL, Miyoshi H, Loh J, Lennerz JK, et al. A key role for autophagy and the autophagy gene Atg16l1 in mouse and human intestinal Paneth cells. Nature 2008;456:259-63.
4. Cadwell K, Stappenbeck TS, Virgin HW. Role of autophagy and autophagy genes in inflammatory bowel disease. Curr Top Microbiol Immunol 2009;335:141-67.
5. Stappenbeck TS. The role of autophagy in Paneth cell differentiation and secretion. Mucosal Immunol 2010;3:8-10.
6. Jung HS, Chung KW, Won Kim J, Kim J, Komatsu M, Tanaka K, et al. Loss of autophagy diminishes pancreatic beta cell mass and function with resultant hyperglycemia. Cell Metab 2008;8:318-24.
7. Ebato C, Uchida T, Arakawa M, Komatsu M, Ueno T, Komiya K, et al. Autophagy is important in islet homeostasis and compensatory increase of beta cell mass in response to high-fat diet. Cell Metab 2008;8:325-32.
8. Galli SJ, Nakae S, Tsai M. Mast cells in the development of adaptive immune responses. Nat Immunol 2005;6:135-42.
9. Galli SJ, Kalesnikoff J, Grimbaldeston MA, Piliponsky AM, Williams CM, Tsai M. Mast cells as "tunable" effector and immunoregulatory cells: recent advances. Annu Rev Immunol 2005;23:749-86.
10. Supajatura V, Ushio H, Nakao A, Akira S, Okumura K, Ra C, et al. Differential responses of mast cell Toll-like receptors 2 and 4 in allergy and innate immunity. J Clin Invest 2002;109:1351-9.
11. Supajatura V, Ushio H, Nakao A, Okumura K, Ra C, Ogawa H. Protective roles of mast cells against enterobacterial infection are mediated by Toll-like receptor 4. J Immunol 2001;167:2250-6.
12. Malaviya R, Abraham SN. Mast cell modulation of immune responses to bacteria. Immunol Rev 2001;179:16-24.
13. Menager MM, Menasche G, Romao M, Knapnougel P, Ho CH, Garfa M, et al. Secretory cytotoxic granule maturation and exocytosis require the effector protein hMunc13-4. Nat Immunol 2007;8:257-67.
14. Logan MR, Odemuyiwa SO, Moqbel R. Understanding exocytosis in immune and inflammatory cells: the molecular basis of mediator secretion. J Allergy Clin Immunol 2003;111:923-32; quiz 33.
15. Komatsu M, Waguri S, Ueno T, Iwata J, Murata S, Tanida I, et al. Impairment of starvation-induced and constitutive autophagy in Atg7-deficient mice. J Cell Biol 2005;169:425-34.
16. Komatsu M, Waguri S, Koike M, Sou YS, Ueno T, Hara T, et al. Homeostatic levels of p62 control cytoplasmic inclusion body formation in autophagy-deficient mice. Cell 2007;131:1149-63.
17. Mizushima N, Yamamoto A, Matsui M, Yoshimori T, Ohsumi Y. In vivo analysis of autophagy in response to nutrient starvation using transgenic mice expressing a fluorescent autophagosome marker. Mol Biol Cell 2004;15:1101-11.
18. Niyonsaba F, Ushio H, Hara M, Yokoi H, Tominaga M, Takamori K, et al. Antimicrobial peptides human beta-defensins and cathelicidin LL-37 induce the secretion of a pruritogenic cytokine IL-31 by human mast cells. J Immunol 2010;184:3526-3534.
19. Kamijo S, Takai T, Kuhara T, Tokura T, Ushio H, Ota M, et al. Cupressaceae pollen grains modulate dendritic cell response and exhibit IgE-inducing adjuvant activity in vivo. J Immunol 2009;183:6087-94.
20. Miyoshi H. Gene delivery to hematopoietic stem cells using lentiviral vectors. Methods Mol Biol 2004;246:429-38.
21. Kuma A, Hatano M, Matsui M, Yamamoto A, Nakaya H, Yoshimori T, et al. The role of autophagy during the early neonatal starvation period. Nature 2004;432:1032-6.
22. Nishida K, Yamasaki S, Ito Y, Kabu K, Hattori K, Tezuka T, et al. Fc{epsilon}RI-mediated mast cell degranulation requires calcium-independent microtubule-dependent translocation of granules to the plasma membrane. J Cell Biol 2005;170:115-26.
23. Metzelaar MJ, Wijngaard PL, Peters PJ, Sixma JJ, Nieuwenhuis HK, Clevers HC. CD63 antigen: a novel lysosomal membrane glycoprotein, cloned by a screening procedure for intracellular antigens in eukaryotic cells. J Biol Chem 1991;266:3239-45.
24. Fader CM, Colombo MI. Autophagy and multivesicular bodies: two closely related partners. Cell Death Differ 2009;16:70-8.
25. Komatsu M, Waguri S, Chiba T, Murata S, Iwata J, Tanida I, et al. Loss of autophagy in the central nervous system causes neurodegeneration in mice. Nature 2006; 441:880-4.
26. Hara T, Nakamura K, Matsui M, Yamamoto A, Nakahara Y, Suzuki-Migishima R, et al. Suppression of basal autophagy in neural cells causes neurodegenerative disease in mice. Nature 2006;441:885-9.
27. Moscat J, Diaz-Meco MT. p62 at the crossroads of autophagy, apoptosis, and cancer. Cell 2009;137:1001-4.
28. Manjithaya R, Anjard C, Loomis WF, Subramani S. Unconventional secretion of Pichia pastoris Acb1 is dependent on GRASP protein, peroxisomal functions, and autophagosome formation. J Cell Biol 2010;188:537-46.
29. Duran JM, Anjard C, Stefan C, Loomis WF, Malhotra V. Unconventional secretion of Acb1 is mediated by autophagosomes. J Cell Biol 2010;188:527-36.
30. Nickel W, Rabouille C. Mechanisms of regulated unconventional protein secretion. Nat Rev Mol Cell Biol 2009;10:148-55.
31. Tiwari N, Wang CC, Brochetta C, Ke G, Vita F, Qi Z, et al. VAMP-8 segregates mast cell-preformed mediator exocytosis from cytokine trafficking pathways. Blood 2008;111:3665-74.
32. Puri N, Roche PA. Mast cells possess distinct secretory granule subsets whose exocytosis is regulated by different SNARE isoforms. Proc Natl Acad Sci U S A 2008;105:2580-5.
33. Dvorak AM. Ultrastructural studies of human basophils and mast cells. J Histochem Cytochem 2005;53:1043-70.
34. Andrews NW. Regulated secretion of conventional lysosomes. Trends Cell Biol 2000;10:316-21.

METHODS

Mice

The $Atg7^{Flox(F)/Flox(F)}$, $Atg7^{F/F}$:*Mx*, $Atg7^{F/F}$:*Mx*:$p62^{+/-}$, and $Atg7^{F/F}$:*Mx*:$p62^{-/-}$ mice were described previously.[E1,E2] C57BL/6 mice were purchased from Japan Clea (Tokyo, Japan). To induce deletion of *Atg7* gene, 8-week-old to 12-week-old $Atg7^{F/F}$:*Mx*, $Atg7^{F/F}$:*Mx*:$p62^{+/-}$, and $Atg7^{F/F}$:*Mx*:$p62^{-/-}$ mice were injected with 300 μg poly I:C (Sigma-Aldrich, Tokyo, Japan) 3 times every other day. At 2 weeks after the first poly I:C injection, BM cells from indicated genotyped mice were prepared as described and used for induction of BMMCs. In parallel experiments, *Mx-cre* negative flox mice were similarly injected with poly I:C, and BM cells were used to generate control BMMCs. Deletion of floxed alleles of *Atg7* genes was confirmed by PCR using BM cells or BMMCs. All experiments were performed according to the guidelines approved by the Institutional Animal Experiments Committee of Juntendo University School of Medicine.

Antibodies

Anti-LC3 (Medical and Biological Laboratories [MBL]), anti–β-actin (Sigma-Aldrich), and anti-p62 (Stressgen) were purchased from indicated sources. Anti-phospho (p)-syk, anti-syk, anti-phospho-PLC-γ1, anti-phospho-gab2, and anti-gab2 were purchased from Cell Signaling technology (Boston, Mass). Rabbit anti-LC3 antibody was generated and described previously.[E2]

Cells

Bone marrow–derived mast cells were generated as previously described.[E3] Briefly, BM cells were cultured in RPMI 1640 medium (Sigma-Aldrich) supplemented with 10% heat-inactivated FCS, 100 μmol/L 2-mercaptoethanol, 10 μmol/L minimum essential medium-nonessential amino acids, 100 U/mL penicillin, 100 μg/mL streptomycin, and 10 ng/mL murine IL-3 (Peprotech) for 5 to 8 weeks. After 5 weeks of culture, more than 98% of cells that were positive for both c-kit and FcεRI on cell surfaces by flow cytometry and Diff-Quick staining were considered to be mature mast cells.

Confocal microscopy

Bone marrow–derived mast cells were plated onto 12 wells containing 60-mm dishes (Ibidi GmbH) pretreated with poly-L-lysine (Sigma-Aldrich) and attached to dishes by centrifugation. Then cells were fixed with 4% paraformaldehyde in PBS for 30 minutes and permeabilized with 50 μg/mL digitonin-PBS for 10 minutes. Cells were immunostained with anti-LC3, antiubiquitin, and anti-p62 antibodies in 1% BSA-Tris-buffered saline for 1 hour and were visualized with Alexa 488–conjugated or 594-conjugated secondary antibodies (Invitrogen). Confocal microscopy was performed on an FV1000 (Olympus, Tokyo, Japan). Pictures were analyzed by FV10-ASW (Olympus).

Western blotting

Bone marrow–derived mast cells were untreated or stimulated as described. After stopping the reaction by adding ice-cold PBS, sample buffer containing SDS was directly added to the pellets, followed by brief sonication. Then, lysates were subjected to SDS-PAGE and transferred onto polyvinylidene difluoride membranes (Millipore). The membranes were analyzed by immunoblotting with indicated antibodies, followed by horseradish peroxidase–conjugated respective secondary anti-immunoglobulin antibodies. The membranes were developed with the Enhanced Chemiluminescence Western Blotting Detection System Plus (GE Healthcare Life Sciences, Tokyo, Japan) and analyzed by LAS4000 (GE Healthcare Life Sciences). Relative intensities of phosphorylated and total proteins were calculated by an ImageGauge (GE Healthcare Life Sciences). To draw kinetics curves of phosphorylated proteins after stimulation, relative ratios of intensities of each phosphorylated protein to those of corresponding total protein were calculated and plotted at indicated times.

Degranulation of mast cells

Bone marrow–derived mast cells were sensitized with 1 μg/mL anti-trinitrophenol (TNP) IgE mAb (clone IgE-3; BD Biosciences) for 1 hour and then suspended at 1×10^6 cells/mL in Tyrode buffer containing 0.1% BSA. Cells were stimulated with indicated concentrations of anti-IgE antibody (BD Bioscience) or 1.6 nmol/L PMA plus 1 μmol/L Ionomycin (Sigma-Aldrich) for indicated times at 37°C. Degranulation of mast cells was determined by β-hexosaminidase and histamine release as described previously.[E3] Degranulation was expressed as net percent release of β-hexosaminidase ([OD: stimulated – unstimulated/OD: total lysate – unstimulated] × 100%). Concentrations of histamine and LTC_4 in the same supernatants were determined by competitive ELISA kit (Oxford Biomedical Research, Inc) according to the manufacturer's instructions. Degranulation was expressed as percent release of histamine as described in β-hexosaminidase.

Measurement of intracellular Ca^{2+} mobilization

Intracellular Ca^{2+} mobilization from BMMCs was measured by a no-washing method using a FLIPR Calcium Assay Kit (Molecular Devices, Sunnyvale, Calif) as previously described.[E4] Briefly, IgE-sensitized BMMCs were seeded at a density of 3×10^5 cells per well into poly-D-lysine–coated 96-well plates (Becton Dickinson, Franklin Lakes, NJ) and loaded with Calcium 3 Reagent (Molecular Devices) containing 2.5 mmol/L probenecid (Sigma-Aldrich) for 1 hour at 37°C. Fluorescence change by addition of agonist was measured by using a FlexStation II (Molecular Devices).

Cytokine measurement of stimulated-BMMCs

IgE-sensitized BMMCs (2×10^6/mL) were stimulated with indicated concentrations of anti-IgE (BD Biosciences) for 6 hours. Concentrations of cytokines in supernatants were determined by using ELISA kit according to the manufacturer's instructions (R & D Systems, Minneapolis, Minn).

Statistical analysis

Statistical analysis was performed by unpaired Student *t* test. $P < .05$ was considered to be statistically significant.

REFERENCES

E1. Komatsu M, Waguri S, Koike M, Sou YS, Ueno T, Hara T, et al. Homeostatic levels of p62 control cytoplasmic inclusion body formation in autophagy-deficient mice. Cell 2007;131:1149-63.

E2. Komatsu M, Waguri S, Ueno T, Iwata J, Murata S, Tanida I, et al. Impairment of starvation-induced and constitutive autophagy in Atg7-deficient mice. J Cell Biol 2005;169:425-34.

E3. Supajatura V, Ushio H, Nakao A, Akira S, Okumura K, Ra C, et al. Differential responses of mast cell Toll-like receptors 2 and 4 in allergy and innate immunity. J Clin Invest 2002;109:1351-9.

E4. Chen X, Niyonsaba F, Ushio H, Hara M, Yokoi H, Matsumoto K, et al. Antimicrobial peptides human beta-defensin (hBD)-3 and hBD-4 activate mast cells and increase skin vascular permeability. Eur J Immunol 2007;37:434-44.

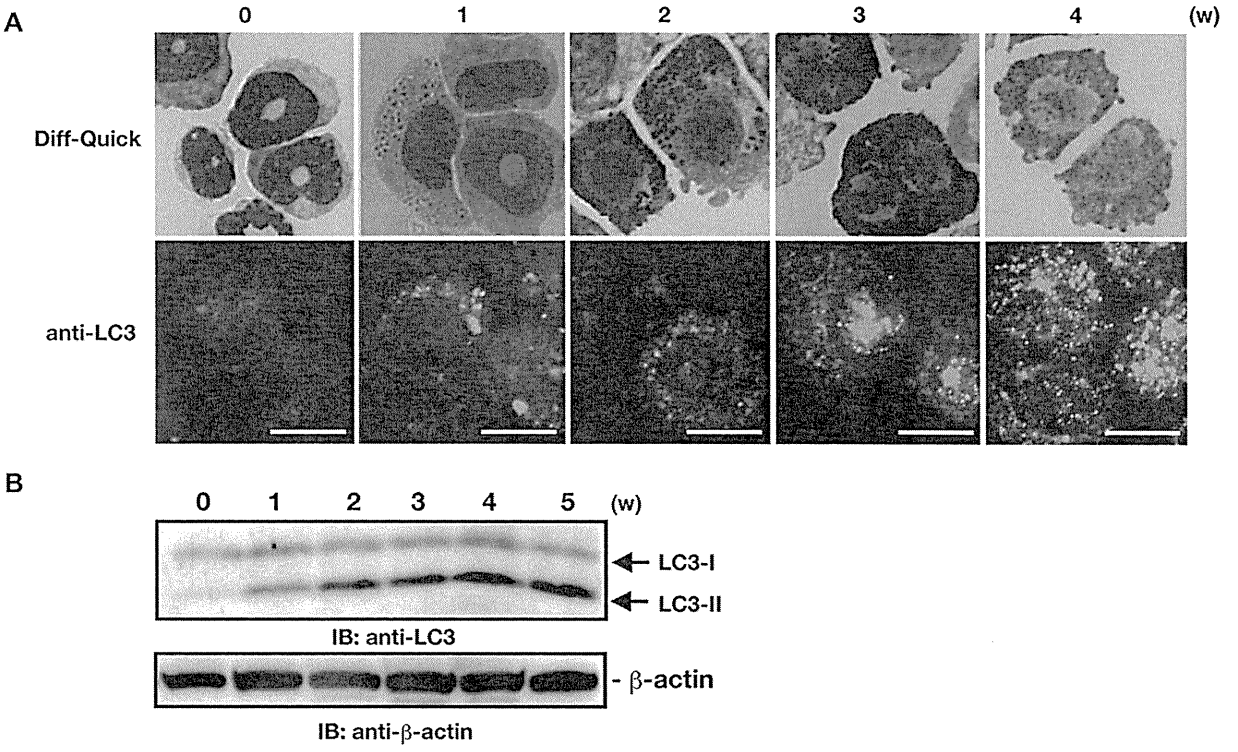

FIG E1. Induction of autophagy is correlated with maturation of BMMCs. **A,** BM-derived cells from wild-type mice were stained with anti-LC3 antibody or Diff-Quick at indicated times after starting culture. Scale bars, 10 μm. *W,* Weeks. **B,** Conversion of LC3-I to LC3-II was analyzed by immunoblotting *(IB).*

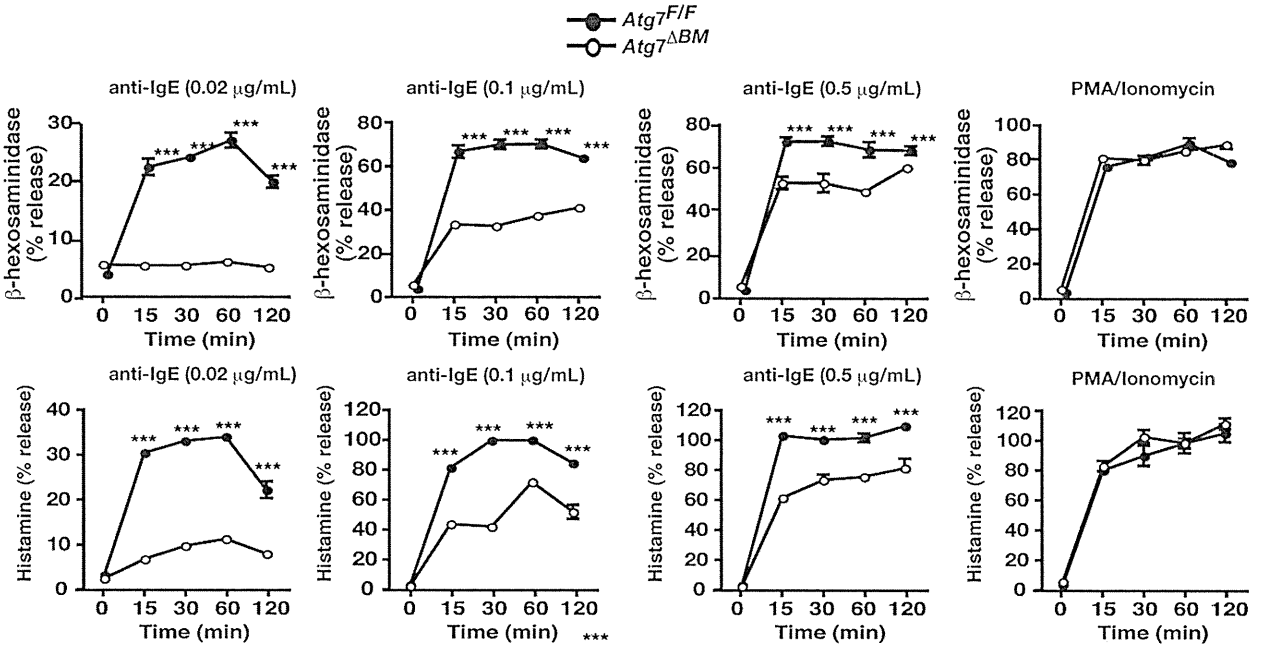

FIG E2. FcεRI-induced degranulation is not delayed but is severely impaired in $Atg7^{\Delta BM}$-BMMCs. Release of β-hexosaminidase and histamine from $Atg7^{F/F}$-BMMCs and $Atg7^{\Delta BM}$-BMMCs at indicated times after stimulation was measured. Results are representative of 2 independent experiments showing means ± SDs of triplicate samples. ***$P < .001$.

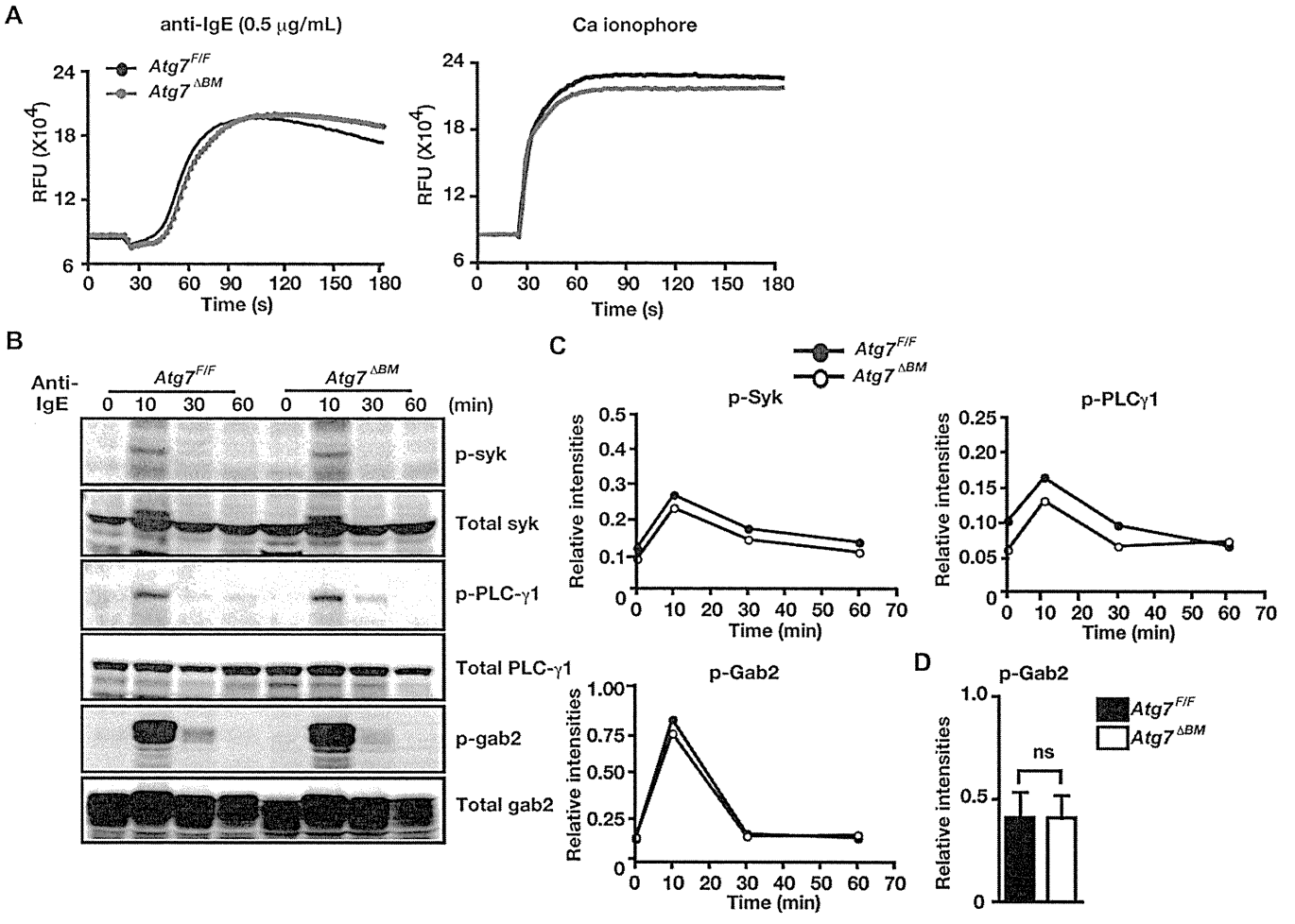

FIG E3. Early signaling events are not impaired in *Atg7*$^{\Delta BM}$-BMMCs. **A,** Ca^{2+} mobilization is not impaired in *Atg7*$^{\Delta BM}$-BMMCs. Results are representative of 3 independent experiments. *RFU,* Relative fluorescence units. **B,** Phosphorylation of early signaling molecules is not impaired in *Atg7*$^{\Delta BM}$-BMMCs. Results are representative of 2 to 3 independent experiments. *p,* Phosphorylated. **C,** Kinetics of relative ratios of intensities of each phosphorylated protein per corresponding total protein. Results are representative of 2 to 3 independent experiments. **D,** Relative ratios of p-Gab2 at 10 minutes after stimulation. Results are means ± SDs of 4 independent experiments. *ns,* Not significant.

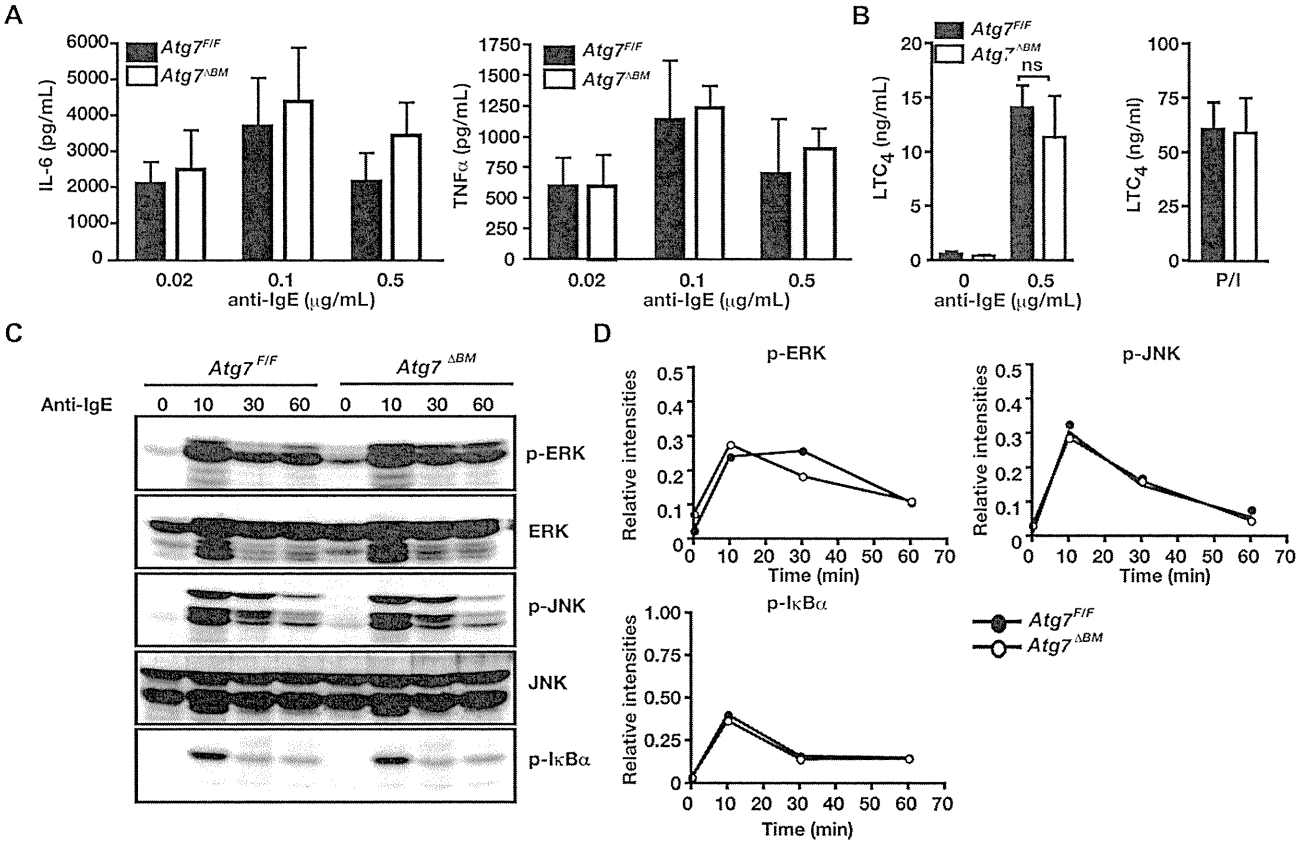

FIG E4. Cytokine release, LTC_4 generation, and phosphorylation of MAPKs are not impaired in $Atg7^{\Delta BM}$-BMMCs. Release of IL-6 and TNF-α **(A)** and generation of LTC_4 by $Atg7^{F/F}$-BMMCs and $Atg7^{\Delta BM}$-BMMCs **(B)**. *P/I*, PMA/ionomycin. Results are means ± SDs of triplicate samples of pooled data of 9 independent experiments or 3 independent experiments, respectively. Phosphorylation of MAPKs in $Atg7^{F/F}$-BMMCs and $Atg7^{\Delta BM}$-BMMCs **(C)**, and kinetics of relative ratios of intensities of each phosphorylated protein per corresponding total protein **(D)**. Results are representative of 2 to 3 independent experiments *ERK*, Extracellular signal-regulated kinase; *JNK*, c-jun N-terminal kinase.

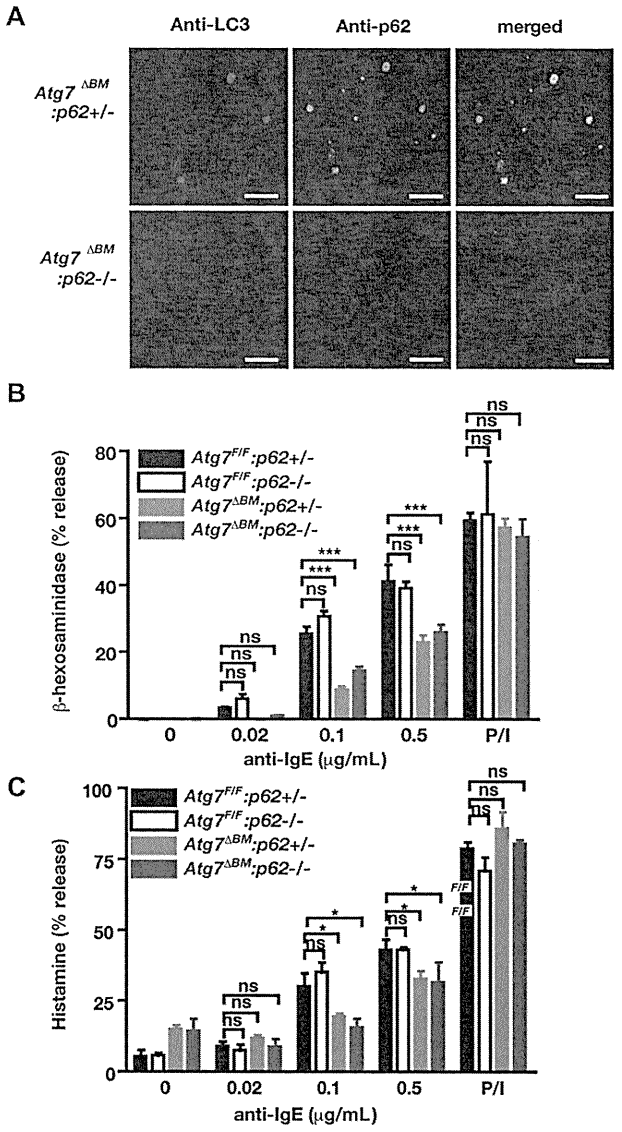

FIG E5. Ablation of p62-containing aggregates does not rescue a defect in degranulation of mast cells. **A,** Confocal microscopic analysis of BMMCs from indicated genotyped mice stained with indicated antibodies. Scale bars, 10 μm. **B,** FcεRI-induced degranulation (release of β-hexosaminidase and histamine) is still impaired in BMMCs from $Atg7^{\Delta BM}$:$p62^{-/-}$ mice. Results are means ± SDs of 3 independent experiments. *$P < .05$; ***$P < .001$. *ns,* Not significant. *P/I,* PMA/ionomycin.

Critical role of transcription factor PU.1 in the expression of CD80 and CD86 on dendritic cells

*Shunsuke Kanada,[1,2] *Chiharu Nishiyama,[1] Nobuhiro Nakano,[1] Ryuyo Suzuki,[1] Keiko Maeda,[1] Mutsuko Hara,[1] Nao Kitamura,[1] Hideoki Ogawa,[1] and Ko Okumura[1,2]

[1]Atopy (Allergy) Research Center and [2]Department of Immunology, Juntendo University School of Medicine, Tokyo, Japan

In this study, we investigated the role of a transcription factor, PU.1, in the regulation of CD80 and CD86 expression in dendritic cells (DCs). A chromatin immunoprecipitation assay revealed that PU.1 is constitutively bound to the CD80 and CD86 promoters in bone marrow–derived DCs. In addition, co-expression of PU.1 resulted in the transactivation of the CD80 and CD86 promoters in a reporter assay. The binding of PU.1 to *cis*-enhancing regions was confirmed by electromobility gel-shift assay. As expected, inhibition of PU.1 expression by short interfering RNA (siRNA) in bone marrow–derived DCs resulted in marked down-regulation of CD80 and CD86 expression. Moreover, overexpression of PU.1 in murine bone marrow–derived lineage-negative cells induced the expression of CD80 and CD86 in the absence of monocyte/DC-related growth factors and/or cytokines. Based on these results, we conclude that PU.1 is a critical factor for the expression of CD80 and CD86. We also found that subcutaneous injection of PU.1 siRNA or topical application of a cream-emulsified PU.1 siRNA efficiently inhibited murine contact hypersensitivity. Our results suggest that PU.1 is a potential target for the treatment of immune-related diseases. (*Blood.* 2011; 117(7):2211-2222)

Introduction

T-cell initiation requires 2 signals from antigen-presenting cells (APCs). The first signal comes from ligation of the T-cell receptor and the major histocompatibility complex (MHC)/antigen presented on the surface of APCs, and the second signal is via additional costimulatory molecules, including the interaction between the CD28 family on T cells and B7, eg, CD80 (B7-1) and CD86 (B7-2), expressed on the APC.[1-3] CD80 and CD86 are members of the immunoglobulin supergene family encoded by separate genes, and are expressed on dendritic cells (DCs) or up-regulated on activated macrophages/monocytes, B cells, and activated T cells.[1-6] CD80 or CD86 can provide costimulatory signals by engaging CD28 or CTLA4 (cytotoxic T-lymphocyte antigen 4; CD152) on T cells. The engagement of CD28 with CD80 or CD86 leads to multiple effects on the immune response, including T-cell activation and differentiation and tissue migration.[7-9]

In contrast to CD28, the outcome of CTLA4 engagement on T cells is to suppress proliferation by transmitting an inhibitory signal.[10] In addition, a subset of T cells with potent immunoregulatory properties, $CD4^+CD25^+$ regulatory T cells, constitutively expresses CTLA4.[11,12] Thus, interactions between CTLA4 and CD80 or CD86 provides an immunosuppressive function in modulating T-cell proliferation and plays a role in immune tolerance. Based on these observations, the regulated expression of costimulatory molecules is critical for immune function. Therefore, revealing the molecular mechanisms of gene expression of costimulatory molecules is essential for an understanding of the regulation of T cell–mediated immune responses.

Despite the importance of CD80 and CD86, the critical transcription factor for gene expression of CD80 or CD86 is still unknown. Transcription factors involved in stimulus-induced expression of CD80 or CD86 have been observed in some promoter structure analyses; for example, interferon regulatory factor 7 (IRF7) regulates lipopolysaccharide (LPS)–induced human CD80 transcription through the activation of Jun N-terminal kinase in monocytes,[13] nuclear factor κ-light-chain-enhancer of activated B cells (NF-κB) plays a role in stimulation-induced transactivation of murine CD80 in B-cell lines,[14] human CD86 in B cells,[15] and CD86 in DCs.[16] However, the specific transcription factors regulating the basic and constitutive expression of CD80 and CD86 have not been identified to date.

PU.1 is a transcription factor belonging to the Ets family, which is involved in hematopoietic cell development. Although PU.1 is required for the development of thymic and myeloid DCs, including some specific gene expression by DCs in the analysis of $PU.1^{-/-}$ animals,[17,18] the effects of PU.1 on the expression of CD80 and CD86 have not been verified in those reports. In our previous studies, mast cells and their progenitors overexpressing PU.1 acquired some DC-specific gene expression, suggesting that PU.1 is a master regulator for gene expression of DCs.[19-21] These findings prompted us to analyze the role of PU.1 in the expression of CD80 and CD86 in DCs. In the present study, we show that PU.1 plays a key role in the gene expression of CD80 and CD86 in granulocyte-macrophage colony-stimulating factor (GM-CSF)–cultured, bone marrow–derived DCs (BMDCs).

Submitted June 17, 2010; accepted November 4, 2010. Prepublished online as *Blood* First Edition paper, November 30, 2010; DOI 10.1182/blood-2010-06-291898.

*S.K. and C.N. contributed equally to this study.

The online version of this article contains a data supplement.

The publication costs of this article were defrayed in part by page charge payment. Therefore, and solely to indicate this fact, this article is hereby marked "advertisement" in accordance with 18 USC section 1734.

Methods

Cells

BMDCs were generated from the femoral and tibial bone marrow cells of female BALB/c mice (Japan SLC) as described previously.[22] All animal experiments were performed according to the approved manual of the institutional review board of Juntendo University School of Medicine, Japan. Cells were incubated in RPMI 1640 (Sigma-Aldrich) supplemented with 10% heat-inactivated fetal calf serum (JRH Biosciences), 100 U/mL of penicillin, 100 μg/mL of streptomycin, 100μM 2-mercaptoethanol, 10μM Minimum Essential Medium nonessential amino acid solution (Invitrogen), and 20 ng/mL of murine GM-CSF (Wako Pure Chemical Industries) at 37°C in a humidified atmosphere in the presence of 5% CO_2. The purity of $CD11c^+$ BMDCs isolated by the MACS separation system with mouse CD11c MicroBeads and an autoMACS (all Miltenyi Biotech) was confirmed to be over 98% by flow cytometry. Lineage-negative (Lin^-) cells were prepared from the femoral and tibial bone marrow cells of female BALB/c mice by the MACS separation system according to the manufacturer's instructions. Briefly, bone-marrow cells were treated with biotinylated monoclonal antibodies (mAbs) against mouse CD5, CD45R (B220), CD11b, Ly-6G (Gr-1), 7-4, and Ter-119. The cell suspension treated with biotinylated mAbs was then reacted with MicroBeads conjugated with anti–biotin mAbs (clone: Bio3-18E7.2; mouse IgG) and was applied to an autoMACS. The purity of the isolated Lin^- cells, which were collected as the negative fraction using this MACS separation system, was over than 95% in FACS analysis. The simian kidney cell line CV-1 was purchased from the RIKEN Cell Bank. CV-1 and the mouse mono-macrophage cell lines RAW264.7 and J774 were maintained in Dulbecco modified Eagle medium (Sigma-Aldrich) with 10% heat-inactivated fetal calf serum, 100 U/mL of penicillin, and 100 μg/mL of streptomycin.

LPS and interferonγ stimulation

Cells were stimulated in the presence or absence of 1 μg/mL of LPS (Sigma) and/or 100 ng/mL of interferonγ (IFNγ; PeproTech).

Flow cytometric analysis

Phycoerythrin (PE)–conjugated anti–mouse antibodies against CD80, CD86, I-Ad, CD11b, and CD11c and fluorescein isothiocyanate (FITC)–conjugated anti–mouse antibodies against CD86, I-Ad, CD11b, CD11c (all of which were purchased from BD Pharmingen); PE-conjugated anti–CD205 (from Miltenyi Biotech); PE-conjugated anti–CD207 and anti–CD209 (eBioscience); FITC-conjugated anti–Toll-like receptor 2 (anti–TLR2) and PE-conjugated anti–TLR4 (BioLegend) were used to stain each cell-surface molecule by incubation for 0.5-1 hour at 4°C after blocking Fc receptors with 2.4G2 (BD Pharmingen). After washing with phosphate-buffered saline, cells were analyzed using a FACSCalibur flow cytometer (BD Biosciences).

5′-rapid amplification of cDNA ends procedure

Total RNA was prepared from BALB/c BMDCs and was used for 5′-rapid amplification of cDNA ends (5′-RACE) with a GeneRacer kit (Invitrogen) according to the manufacturer's instructions. Briefly, total RNA was treated with calf intestinal phosphatase to remove the 5′ phosphates, and the product was then treated with tobacco acid pyrophosphatase to remove the 5′ cap structure. The decapped mRNA was ligated with the GeneRacer RNA oligo and reverse-transcribed using random primers. To obtain 5′ ends, the first-strand cDNA was amplified using the following primers: forward primer, GeneRacer 5′ primer (Invitrogen); reverse primers, CD80-R1 (5′-TCCACCCGGCAGATGCTA-3′), CD80-R3 (5′-TCCACCCGGCAGATGCTA-3′), and CD86-R1 (5′-TCCACCCGGCAGATGCTA-3′). To confirm that these polymerase chain reaction (PCR) products were indeed the expected products, nested PCR was performed with the following primers: forward primer, GeneRacer 5′ Nested primer (Invitrogen); reverse primers, CD80-R1-nest (5′-TCCACCCGGCAGATGCTA-3′), CD80-R2 (5′-TCCACCCGGCAGATGCTA-3′), and CD86-R1-nest (5′-TCCACCCGGCAGATGCTA-3′). TOPO (Invitrogen) cloning was the performed with PCR products, and the products were sequenced.

Quantitative reverse-transcriptase PCR

Total RNA was isolated from each cell or ear tissue with the RNeasy Mini Kit or the RNeasy Lipid Tissue Mini Kit (QIAGEN) per the supplier's instructions, and was used as a template for reverse transcription. Reverse transcription to synthesize cDNA for CD80-1, CD80-2, CD80-common, CD86-1, CD86-2, CD86-common, and β-actin was performed using high-capacity cDNA reverse-transcription kits (Applied Biosystems) or the ReverTra Ace qPCR RT kit (TOYOBO). Quantitative PCR was performed using TaqMan Universal PCR Master Mix (Applied Biosystems) and a 7500 real-time PCR system with TaqMan gene expression assays of mouse target genes,[23] including CD80 (Mm00711660-m1), CD86 (Mm00444543-m1), and an endogenous control (β-actin), and the primers and TaqMan probes listed in supplemental Table 1 (available on the *Blood* Web site; see the Supplemental Materials link at the top of the online article). The expression levels of CD80-1, CD80-2, CD80-common, CD86-1, CD86-2, and CD86-common are given relative to those of β-actin by calculation of the cycle threshold values in amplification plots with 7500 SDS software Version 1.2.2 (Applied Biosystems), as recommended by the supplier.

Chromatin immunoprecipitation assay

A chromatin immunoprecipitation (ChIP) assay was performed using a kit (Upstate Biotechnology) as described previously.[24] Anti–PU.1 goat IgG antibody (D19; Santa Cruz Biotechnologies), anti–NF-kB rabbit IgG (C-20; Santa Cruz Biotechnologies), anti–IRF4 goat IgG antibody (M17; Santa Cruz Biotechnologies), rabbit IgG (Sigma), and goat IgG (Sigma) were used. The amount of chromosomal DNA immunoprecipitated by each antibody was determined by quantitative PCR. Primers and TaqMan probe sequences used for this analysis are as listed in supplemental Table 2. The amount of target DNA bound with PU.1, NF-κB p65, or IRF4 was quantified from the cycle threshold value, which was determined with 7500 SDS software (Applied Biosystems). Briefly, the ratio of a specific DNA fragment in each immunoprecipitate to that fragment in the DNA before immunoprecipitation (input DNA) was calculated from each cycle threshold value.

Plasmid construction

A series of murine CD80 or CD86 promoter fragments were amplified from murine genomic DNA purified from BALB/c mice by PCR. Primers with restriction endonuclease recognition sequences are synthesized as listed in supplemental Table 3. Amplified PCR products were subcloned into the pCR4-TOPO vector, and the nucleotide sequences were confirmed. The correct insertions were subcloned into the *Xho*I/*Hin*dIII- or *Xho*I/*Bgl*II-digested pGL4.10 (Promega), the basic luciferase reporter plasmid, to generate 4 reporter plasmids, pGL4.10-CD80-1, CD80-2, CD86-1, and CD86-2. A series of reporter plasmids with various lengths of each promoter were generated by introduction of *Xho*I recognition sequences by site-directed mutagenesis using a QuikChange site-directed mutagenesis kit (Stratagene). The 5′-region of *Xho*I-sequence-introduced each promoter was removed by *Xho*I digestion and subsequent self-ligation, resulting in the generation of 5′-deleted promoter plasmid.

To generate the IRF4 expression plasmid pCR-IRF4, mouse IRF4 cDNA (NM_013674) amplified by PCR using 5′-GCACGCGTCATGAACTTGGAGAC-3′ and 5′-CGGCTGCCCTGTCAGAGTATTTC-3′ as primers and cDNA synthesized from total RNA of RAW264.7 cells as a template, respectively, was cloned into pCR3.1 (Invitrogen). Other expression plasmids, pCR-PU.1[25] and pCR3.1-IRF8,[26] have been generated in our previous studies. The cDNA encoding the Ets domain (DNA-binding domain) of PU.1 was amplified from pCR-PU.1 by PCR using 5′-GGGGAG*GAATTC*AGCAAGAAGAAGATTCGT-3′, and 5′-GT*CTCGAG*CTAAGAACTGAGTGGAGACAC-3′ (*Eco*RI and *Xho*I recognition sequences are italic) as primers, and PU.1 cDNA of pMX-puro-PU.1[19] was replaced with the PU.1 Ets domain by *Eco*RI/*Xho*I digestion and ligation,